Reliability Engineering and System Safety 272 (2026) 112668

Contents lists available at ScienceDirect

Reliability Engineering and System Safety

journal homepage: www.elsevier.com/locate/ress

Integrated simulation and network analysis of battery fire risk in underground mining systems

Sultan Elcin Eroglu *, Muhammed Kahraman, H. Sebnem Duzgun

Mining Engineering, Colorado School of Mines, 1500 Illinois St., Golden, CO 80401, United States

A R T I C L E I N F O

Keywords:
Battery-electric vehicles
Underground mining
Fire risk
System dynamics
Reliability modeling
Network analysis
Safety systems

A B S T R A C T

The global mining industry is increasingly adopting battery-electric vehicles (BEVs) to meet sustainability goals and reduce emissions; however, their integration introduces new risks, lithium-ion battery fires in confined underground environments. These fires, often triggered by mechanical, thermal, or electrical abuse, escalate rapidly and release toxic gases. This study evaluates BEV fire risks in underground mines using a system safety perspective within a dynamic reliability modeling framework. An integrated framework combining system dynamics modeling (SDM) with HaulSim and VentSim simulations captures interactions among operational practices, environmental stressors, and feedback loops. Simulation outputs feed a regression-based fused model to predict fire probability and assess prevention strategies. Applied to a real-world case at the Turquoise Ridge Underground Mine in Nevada, the SDM comprised 68 components linked by 17,360 feedback loops. Network analysis revealed removing five critical nodes drastically reduced system connectivity. HaulSim results showed cycle times of 13–40 min and depth of discharge above 0.80, indicating short-circuit potential, while VentSim analysis demonstrated lower thermal stress in fully electrified fleets. Annual battery fire probability ranged from 0.10 to 0.29, depending on fleet composition. A five-tier prevention framework reduced risks by up to 99%, emphasizing scenario-dependent strategies to enhance system resilience and mitigate cascading failures.

1. Introduction

The global mining industry is undergoing a significant transformation as operations increasingly transition toward electrification to meet sustainability goals, reduce greenhouse gas emissions, and improve underground working conditions [1]. One of the most significant shifts has been the adoption of battery-electric vehicles (BEVs) in underground mines, replacing traditional diesel-powered fleets [2]. A leading example of this trend is the Macassa gold mine in Ontario which became the first mine in the world to integrate lithium-ion battery--operated trucks and loaders into its underground operations. Beginning in 2012 with an initial fleet of nine battery-powered trucks and 24 loaders, Macassa now conducts approximately 80% of its underground production using BEVs [3]. This transition demonstrates the industry's growing reliance on electrification technologies and highlights the operational and environmental benefits that BEVs can provide. They are significantly more energy-efficient than conventional vehicles, converting about 70–90% of the electricity stored in their batteries into kinetic energy [4]. Since they operate without combustion, BEVs produce no tailpipe emissions, eliminating carbon dioxide (CO_2), nitrogen oxides (NO_x), particulate matter, and other harmful pollutants associated with diesel engines [4]. This not only reduces the environmental footprint of mining operations but also improves underground working conditions by lowering the levels of toxic gases, heat, and noise, contributing to a safer and healthier environment for miners [2].

Despite these advantages of BEVs, they introduce new challenges to the underground mine environments, which affect not only safety but also operational performance and planning. Productivity, for example, becomes closely tied to factors such as the chosen battery charging or swapping strategy, the location and accessibility of charging infrastructure, and the overall mine layout [5]. Additional challenges arise from considerations of economic viability, user-friendliness, battery fire risk, and electrical-related issues [2,6]. Among these challenges, however, the increased risk of battery fires stands out as one of the most critical concerns in underground mines, where confined spaces, restricted ventilation pathways, and limited evacuation routes can quickly escalate a localized incident into a major hazard [7,8]. Because the nature of battery fires differs significantly from conventional diesel

* Corresponding author.
E-mail address: eroglu@mines.edu (S. Elcin Eroglu).

https://doi.org/10.1016/j.ress.2026.112668
Received 22 October 2025; Received in revised form 18 March 2026; Accepted 28 March 2026
Available online 29 March 2026
0951-8320/© 2026 Elsevier Ltd. All rights reserved, including those for text and data mining, AI training, and similar technologies.

vehicle fires, with rapid escalation, high temperatures, potential for reignition after extinguishing open flames, and the potential release of toxic gases, all of which complicate suppression efforts and emergency response [7,8]. These challenges, layered onto an environment already characterized by human, technical, and operational complexities, make underground mines even more complex systems to manage [7,9].

Therefore, as underground mines increasingly adopt BEVs, it has become essential to understand how operational conditions and environmental stressors affect the risk of lithium-ion battery fires and the overall safety of these complex systems over time. This is because lithium-ion battery fires often occur due to mechanical, thermal, or electrical abuse [10]. These abuse mechanisms may be encountered when vehicle collisions, humidity, temperature increases, overcharging or over-discharging of the batteries, or degradation over mining cycles occur [8]. However, despite growing awareness of these mechanisms, limited real-world data, the complex structure of the underground mine environment, and the dynamic nature of mine operations make assessing the risk of battery fires challenging. These challenges underscore the need for a system safety approach, a framework that examines the entire system, including its components and their interactions, to mitigate safety risks that can arise from problematic interactions, even when individual components have not failed [7,9]. By focusing on how these interactions and the dynamic nature of the underground mine systems impact lithium-ion battery fire hazards, a system safety approach enables a deeper understanding of (i) how battery stress develops, (ii) how fire risk evolves dynamically, and (iii) how targeted prevention and mitigation strategies can be designed.

This study presents an integrated modeling framework (IMF) that couples system dynamics modeling (SDM) with mine operational (HaulSim) and underground environmental (VentSim) simulations to analyze how operational and battery-related parameters (cycle times, CT; cycle count; CC, battery swapping frequency, BSF; depth of discharge, DoD) and environmental factors (temperature, ventilation conditions) influence lithium-ion battery fire risk evolution in underground mines adopting BEVs. SDM captures the interactions among key system components and the evolution of fire probability over time, while HaulSim and VentSim simulations provide the operational and thermal inputs that influence battery stress and the potential for fire initiation [11–13]. We obtained values of operational parameters (CT, CC, production rate) and battery-related parameters (DoD, BSF) from HaulSim. Similarly, we acquired the underground environmental conditions (ambient temperature and ventilation patterns) using VentSim models, which are critical factors in battery fire behavior underground.

To demonstrate the application of the IMF, we considered the case of a battery fire that occurred at the Turquoise Ridge Underground Mine. As one of the few documented cases of a BEV fire in an underground mine, this case provides an opportunity to explore how feedback loops within a BEV-integrated underground mine system can lead to battery fires.

This study advances dynamic reliability modeling and system safety in three keyways. First, it introduces a coupled simulation framework integrating system dynamics modeling with domain-specific operational, battery-related (HaulSim) and environmental (VentSim) simulations for underground mining, extending prior applications in chemical, nuclear, and transportation systems [14–16]. This integration enables time-dependent quantification of how operational decisions (e.g., CT, CC, BSF, DoD) propagate to influence fire probability, a capability absents in static fault- and event-tree methods commonly used in mining safety [17,18]. Second, network analysis is applied to identify dominant feedback structures driving battery fire risk, building on complex system vulnerability research [19] and extending beyond component-level reliability analysis to capture emergent system-level hazards [20]. Third, the framework is validated through reconstruction of an actual battery fire incident at the Turquoise Ridge Mine, consistent with system-theoretic accident analysis approaches [21,22]. Together, these contributions support probabilistic safety assessment and evidence-based risk prevention under operational uncertainty. Fourth, a regression-based fused fire probability model (FPM) is developed using simulation- and system dynamics-derived outputs to quantitatively predict fire risk and evaluate the effectiveness of fire prevention strategies under varying environmental and battery-related conditions.

2. The integrated modeling framework (IMF)

The IMF is based on a system-level dynamic analysis of how fire risk evolves in complex underground environments. Instead of focusing only on individual faults in the events or static risk factors, the approach examines how multiple interacting components, such as equipment condition, operational practices, environmental conditions, monitoring efforts, maintenance activities, or managerial activities, collectively influence the likelihood of fire occurrence over time. By capturing the feedback relationships among these components, the IMF allows for a holistic understanding of the system's dynamic behavior and the mechanisms that amplify or suppress fire risk.

As represented in Fig. 1, the IMF consists of four main steps: analysis of system dynamic behavior, development of fire prevention strategies, evaluation of these strategies, and identification of the best-performing prevention strategies.

The first step, analysis of system dynamic behavior, focuses on understanding the system's underlying structure and feedback mechanisms. In this step, SDM is adopted to unpack the complex interdependencies governing battery fire risk in underground mining operations. SDM is used to analyze and solve the problems in complex systems, depending on time, such as water resources management, risk analysis, and analyses of global changes, engineering [23,24]. It is utilized to capture causal relationships, time delays, and feedback loops within complex systems [25]. SDM has been utilized in the field of system safety to examine safety policy proposals and organizational accidents [26]. For instance, a qualitative analysis of organizational safety status was conducted using causal loop diagrams (CLD)-based safety archetypes. This analysis focused on how individual decisions made in various organizational panes can combine to have an adverse and frequently unanticipated impact on safety [26]. Westray mine disaster was analyzed using stock-flow diagrams (SFD) to examine the organizational factors in this disaster [27]. To assess decision rules inherent in the development of exploration systems and to look for potential organizational SDM was presented [26].

SDM consists of CLD, which qualitatively illustrate the cause-and-effect relationships and feedback structures within the system, and stock-flow diagrams (SFDs), which provide a quantitative representation that enables simulation and analysis of how system variables change over time [25].

To initiate this process, the safety-related and battery fire-related components of the underground mining system, along with their interrelationships, are identified and represented through a conceptual CLD. The CLD captures the qualitative relationships among variables such as battery condition, maintenance practices, operational, and environmental conditions, revealing the reinforcing and balancing feedback loops that drive the system's dynamic behavior. Following the development of the CLD, graph analytics techniques including node degree (to identify the most connected variables), clustering coefficient (to measure the tendency of variables to form tightly linked groups), community structure (to detect clusters of interrelated factors), giant connected component analysis (to assess overall system connectivity), and betweenness centrality (to determine key variables that mediate interactions within the system) are applied to evaluate the structural characteristics of the CLD quantitatively.

Based on the causal relationships identified in the CLD, an SFD is then developed to quantify these relationships and calculate the temporal evolution of fire probability. The SFD incorporates the key components that influence fire probability and enables the simulation of

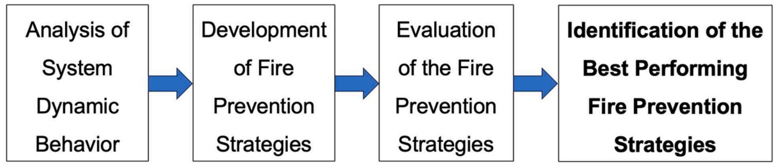

Fig. 1. Steps of the IMF.

their dynamic changes by integrating operational and environmental parameters. Since these parameters, such as equipment utilization, energy consumption, air temperature, and ventilation efficiency, directly affect fire probability, the relevant datasets are generated through HaulSim and VentSim simulations for different operational and environmental scenarios. The simulation outputs are then embedded into the SFD to evaluate how the system behaves under varying conditions dynamically. Through the combination of the CLD and SFD, the system's dynamic structure is analyzed, providing a comprehensive understanding of how interactions among components influence fire probability and how this probability evolves over time in response to operational and environmental changes.

The second step, development of fire prevention strategies (Fig. 1), builds upon the findings from the first step. The dynamic relationships identified in the system model deliver insights into the key leverage points and feedback loops that most strongly affect fire probability. Based on this understanding, a set of fire prevention strategies is formulated, addressing both component-level and system-level improvements. Component-level strategies focus on technical enhancements, such as improved battery management systems, early fault detection, and optimized thermal management. System-level strategies, on the other hand, target broader organizational and operational interventions, including enhanced maintenance scheduling, ventilation control optimization, and emergency response planning.

In the third step, evaluation of fire prevention strategies (Fig. 1), the fire probability results derived from the SFD are used to assess how different prevention strategies influence system behavior under varying operational and environmental conditions. This step focuses on analyzing the dynamic relationships between key parameters such as CT, temperature, and DoD to understand how each strategy alters their interaction within the system. The evaluation also involves examining how the integration of these strategies modifies feedback loops and interconnections identified in the CLD, thereby providing insight into their overall impact on safety performance.

Finally, in the fourth step, identification of the best-performing fire prevention strategies (Fig. 1), the results of the strategy evaluations are synthesized to determine which interventions most effectively maintain system safety and prevent or mitigate the consequences of battery fires. The strategies are ranked based on their performance in reducing fire probability, improving system stability, and minimizing potential losses under critical conditions. The outcomes of this step provide a decision-support foundation for selecting and implementing optimal prevention measures in real underground BEV operations.

Overall, the proposed IMF provides a novel analytical approach to developing, evaluating, and prioritizing safety strategies that ensure the integration of BEVs in underground mines is resilient and sustainable.

3. Implementation of the IMF

To demonstrate the implementation of the IMF, we have chosen the case study of the Turquoise Ridge underground mine BEV fire, previously investigated in [7]. Turquoise Ridge is an underground gold mine located in Nevada, United States. The operation utilizes drift-and-fill and sill benching techniques, incorporating various ramp and shaft systems that link production areas. Since 2020, it has been generating roughly 2700 tonnes of ore daily and operates in two shifts each day. To improve sustainability and facilitate anticipated production increases, the mine began integrating Battery Electric Vehicles (BEVs), specifically Sandvik Z50 haul trucks, in February 2020, without requiring significant modifications to its existing infrastructure [7]. On October 15, 2021, a battery fire occurred during the transit of a battery from the surface to the underground, instigated by a low-impedance and isolation fault [7]. The battery's chemistry consisted of lithium-iron phosphate (LFP). This case establishes a basis for developing realistic scenarios and examining the evolution of battery fire risk under varying conditions, including different equipment fleets and durations in underground mines, by reconstructing the mine's layout and operational context using literature and Mine Safety and Health Administration (MSHA) reports related to the battery fire incident, while also identifying strategies for prevention and mitigation [2,7,28–30]. To assess the battery fire risk for this Turquoise Ridge case, the steps of the IMF described in the previous section were followed.

3.1. Analysis of system dynamic behavior

To analyze the system's dynamic behavior at the Turquoise Ridge Mine (TRM), SDM was applied as the first step in the IMF. This step aims to establish a structured understanding of the system by combining conceptual modeling and simulation-based analysis. As illustrated in Fig. 2, the SDM process consists of three interrelated components: (a) the development of a CLD, (b) simulations conducted using HaulSim and VentSim, and (c) the construction of an SFD.

The CLD was first developed to qualitatively identify the key system components and their interactions within the TRM case. The diagram was then analyzed using graph analytics to examine the system structure, with particular emphasis on communication and interaction mechanisms among production, safety, maintenance, and inspection (enforcement) functions, as well as the feedback loops governing these relationships. The results of this network-based analysis were used in the subsequent step of the IMF to inform the development of the fire prevention strategy, rather than as direct simulation inputs.

Based on the conceptual structure revealed by the CLD analysis and considering data availability, the quantifiable parameters required to estimate battery fire probability were identified. These parameters represent operation under improper working conditions, including abnormal operational and environmental conditions and wear-related

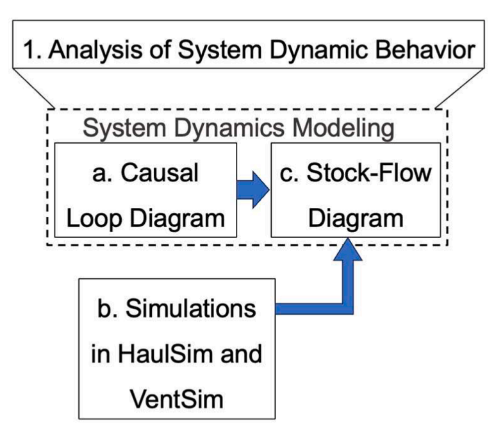

Fig. 2. The first step of IMF: analysis of system dynamic behavior.

degradation associated with manufacturing-related aging. The probabilities of abnormal operational and environmental conditions affecting battery performance were derived from HaulSim and VentSim simulation outputs, which provided time-dependent inputs for the SDM framework. These inputs were integrated into an SFD to evaluate the evolution of battery fire probability over time in the TRM case. Also, a sensitivity analysis was conducted to assess the fire probability's sensitivity to the coupling parameters. Detailed descriptions of the CLD development, simulation modeling, and SFD formulation and outputs are presented in the following sections.

3.1.1. Causal loop diagram (CLD)

The CLD for the TRM case was constructed to depict all the system's components and illustrate their interactions. CLDs are more crucial to comprehending system behavior in the context of SDM than the individual elements of system structure [23]. The CLDs visually organize the components of the system's relationships through two types of causal links: positive and negative linkages. Positive linkages indicate that an increase in the cause variable leads to an increase in the effect variable, or vice versa. Negative linkages represent relationships where an increase in the cause decreases the effect, or vice versa [25]. By connecting these components via negative or positive linkages, feedback loops are formed, which can be either reinforcing or balancing [25]. Reinforcing feedback loop speeds up systemic change, which ultimately leads to either rapid growth or quick decline [23]. Balancing feedback loops exhibit goal-seeking behavior and resist change [23]. When negative or positive connections determine the relationships between all components, these feedback loops are combined, and CLDs emerge. CLDs demonstrate how system components interact to create feedback loops and how these feedback loops interact to define the system's structure [23].

According to [9,7], equipment or vehicle related fires are closely associated with the safety and health, maintenance, production, and managerial performances. Therefore, the CLD of the TRM was created in Stella to see how the interconnected factors influencing the fault probability of the equipment (lithium-ion battery) or vehicle (BEVs), battery fire probability, and overall safety in TRM operations (Fig. 3).

The diagram in Fig. 3, integrates operational activities such as maintenance, training, inspections, and emergency preparedness, as well as organizational elements like regulatory compliance and management commitment. It visually organizes their relationships through positive and negative linkages. Positive linkages are shown in blue, and negative linkages are shown in pink in this diagram. There are 68 different components and 17,360 feedback loops in the CLD of TRM. 8874 of these feedback loops are balancing loops, and 8486 of them are reinforcing loops.

Each component in the CLD represents a critical factor influencing system safety and the risk of lithium-ion battery fires in the TRM. These components can be grouped into several functional categories that reflect both operational activities and organizational influences within the system.

Maintenance-related components include Training, Preventive Maintenance Done, Predictive Maintenance Done, Corrective Maintenance Done, and Emergency Maintenance Done. The 'Training' component specifically refers to maintenance-related training provided to miners, ensuring they are prepared to respond appropriately in the

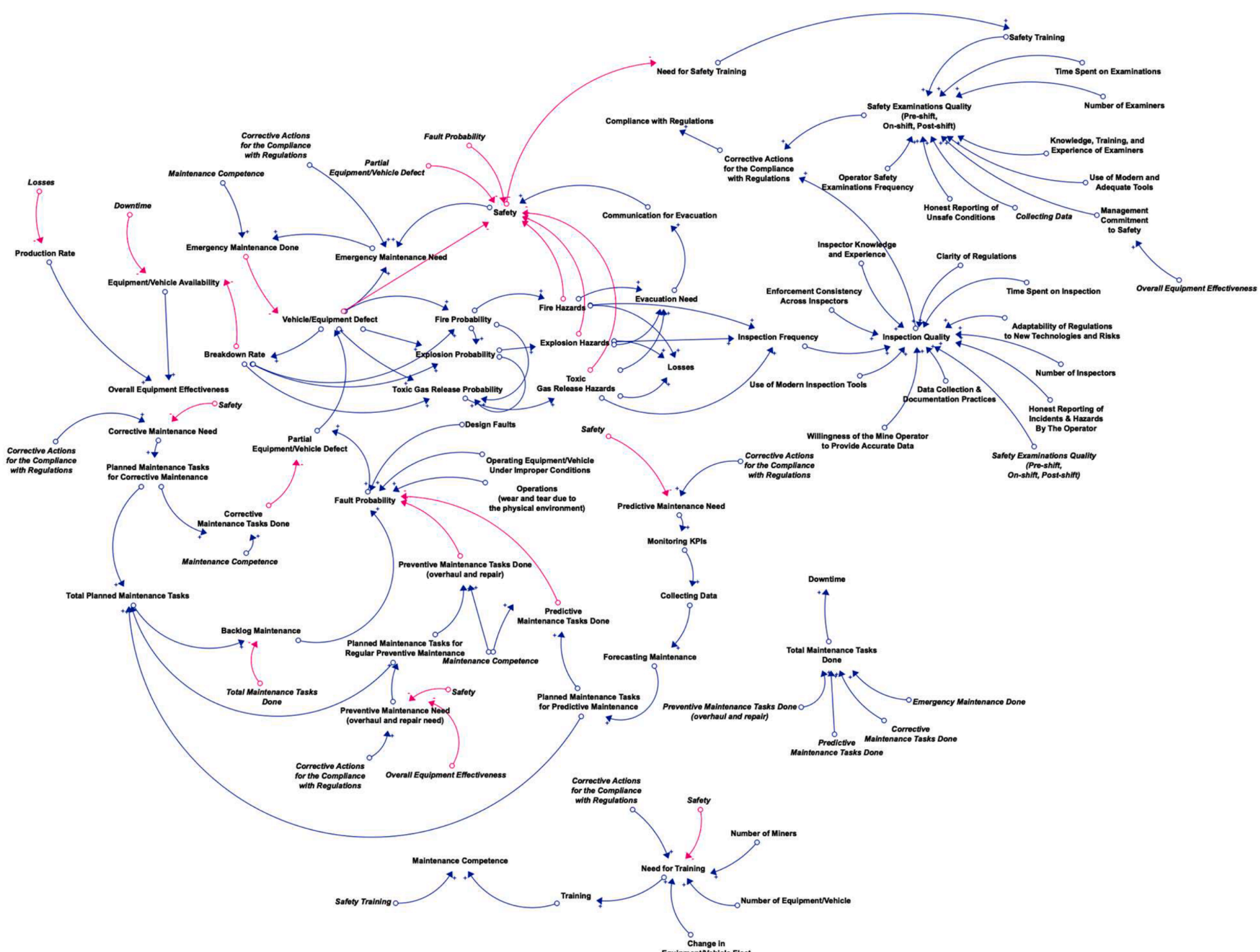

Fig. 3. CLD of the BEV-integrated underground mine environment.

event of emergencies, especially when new equipment or vehicles are introduced, new miners are onboarded, or the equipment fleet undergoes changes. The Preventive, Predictive, Corrective, and Emergency maintenance components encompass different types of maintenance activities performed before or after equipment faults occur. Although these maintenance types look similar, they are different. Repairing, replacing, and maintaining equipment to prevent unplanned faults while in use is known as preventive maintenance [31]. Predictive maintenance is a condition-based maintenance strategy in which equipment is serviced only when measurable signs of deterioration, such as changes in temperature, vibration, noise, lubrication, or corrosion, indicate that maintenance is necessary. This allows interventions to be performed just before a fault occurs [31]. After a fault occurs while the system is operating or after an inspection reveals a failure while the system is not in use, corrective maintenance is performed [31]. On the other hand, emergency maintenance is an unplanned repair activity that must be performed immediately to address sudden equipment faults or hazardous conditions, leaving minimal time for preparation or planning [31]. These represent the operational processes aimed at maintaining equipment health and preventing faults.

Safety-related components cover elements such as 'Safety Examination Quality', 'Safety', 'Safety Training', 'Fire Probability', 'Explosion Probability', 'Toxic Gas Release Probability', 'Losses', 'Evacuation Need', 'Fault Probability', and 'Equipment/Vehicle Defect'. 'Fault Probability' refers to lithium-ion battery fault probability, which may increase due to the design faults of the manufacturer, wear and tear, and operating under improper conditions, such as without proper maintenance, for long CT, allowing the batteries' internal temperature to heat up, or using it with deep discharge rates. If this fault probability does not decrease with the predictive pr preventive maintenance, then it may turn into a defect. The 'Vehicle/Equipment Defect' component specifically refers to defects occurring in BEVs or in the lithium-ion batteries themselves, which are central to concerns about battery fire risk. These components reflect procedures and conditions directly related to hazard detection and mitigation. In particular, the 'Safety' component represents overall system safety, encompassing miner wellbeing, mine infrastructure integrity, equipment condition, and operational continuity. 'Losses' component includes the potential losses such as loss of life, equipment, damage to equipment, injuries, mine infrastructure damage, environmental pollution, or loss of production which may occur after a battery fire.

Inspection and regulatory related components include 'Inspection Quality', 'Corrective Actions for the Compliance with Regulations', and 'Inspector Knowledge and Experience', capturing the system's monitoring and enforcement mechanisms. While 'Safety Examination Quality' and 'Inspection Quality' may appear similar, they serve distinct roles: Safety examinations are conducted regularly by trained personnel within the mining company to identify risks and implement corrective actions based on internally collected data, whereas inspections are performed by external regulatory bodies such as MSHA to ensure compliance with enforced regulations [32,33].

Finally, broader organizational components such as 'Management Commitment to Safety' and 'Overall Equipment Effectiveness' influence multiple subsystems by shaping both operational practices and regulatory compliance efforts. Overall Equipment Effectiveness (OEE) is a key performance indicator that measures how effectively equipment contributes to productive time by combining availability, performance efficiency, and quality rate. In underground mining, OEE is closely tied to management's commitment to safety and maintenance. Effective safety practices and well-planned maintenance reduce downtime, prevent accidents, and enhance system reliability. As a result, improving safety and minimizing interruptions directly increase OEE, supporting a safer and more efficient mining operation [31].

By explicitly mapping these components with the positive or negative linkages, the CLD provides a structured and comprehensive overview of how specific activities and strategies interact to shape system behavior and safety outcomes in underground mining operations. The diagram also highlights the role of inspection activities, training quality, and regulatory enforcement. Improvements in inspection quality, driven by factors such as inspector knowledge and data collection, have a balancing influence on the system by identifying risks earlier and reducing the likelihood of faults and fires. Training and safety examinations also enhance maintenance competence and maintenance tasks done, contributing to system safety through balancing effects.

3.1.2. Analyzing the CLD with graph analytics

After developing the CLD, graph analytics methods were applied in Python to examine the structural properties of the CLD quantitatively. The CLD was first converted into a directed network, where nodes represent system components and edges reflect causal relationships between them, positive and negative linkages, as shown in Fig. 4.

As shown in Fig. 4, the green edges represent positive linkages, while the red edges represent negative linkages between the system components. The nodes shown with blue circles represent the system components.

The first step involved analyzing node degree to identify the most connected and potentially influential components within the system [34]. The result of the node degree analysis is given in Fig. 5.

Fig. 5 represents that the node with the highest degree was 'Inspection Quality' with 14 connections, followed by 'Safety' with 13, and 'Safety Examinations Quality (Pre-shift, On-shift, Post-shift)' with 11. Nodes such as 'Vehicle/Equipment Defect' and 'Fault Probability' both showed degrees of eight. At the same time, 'Toxic Gas Release Hazards' and 'Corrective Actions for Compliance with Regulations' each had seven connections. These results indicate that inspection processes, safety examinations conducted by the mining companies' competent personnel, and maintenance-related factors aimed at preventing or repairing equipment defects play a central role in system safety.

Secondly, the average local clustering coefficient of this network, which measures the likelihood that a node's neighbors are also connected, was calculated to be approximately 0.021 [35]. The distribution of the local clustering coefficient and the average local clustering coefficient of this network are shown in Fig. 6.

As shown in Fig. 6, this low average local clustering coefficient value suggests that the network has a sparse, hierarchical structure rather than tightly clustered groups, which is expected in systems where distinct functional areas are connected through key bridging nodes rather than dense interlinkages.

Community detection was performed using the Louvain method, adapted for directed networks, which revealed distinct communities across 68 elements. These communities aggregated system components with enhanced internal connectivity [36], and are shown in Fig. 7.

In Fig. 7, each community is represented by a different color in the CLD. For example, one cluster focuses on emergency maintenance, fire, safety, and evacuation processes, while other centers focus on preventive maintenance tasks, total maintenance tasks, backlog maintenance, and fault probability. A third group contains inspection quality, regulatory enforcement, and data collection elements. Notably, an overlap was observed between the last two communities, which grouped production-related and regulation-related attributes. This overlap reflects nodes or connections that link operational performance and regulatory compliance, highlighting how certain elements simultaneously influence both domains. Since these two communities share a node, and the previous community has only two nodes, they were combined. As a result, there are six communities in this system. Detecting the communities within the system is essential because connecting those communities to the feedback loops increases the system's resiliency, which, in the context of BEV fire risk, refers to the system's ability to anticipate, absorb, and recover from fire-related disruptions without cascading failures or prolonged operational downtime.

Then, the system's giant connected component (GCC) using strongly connected components (SCC) was detected [37]. The GCC represents the

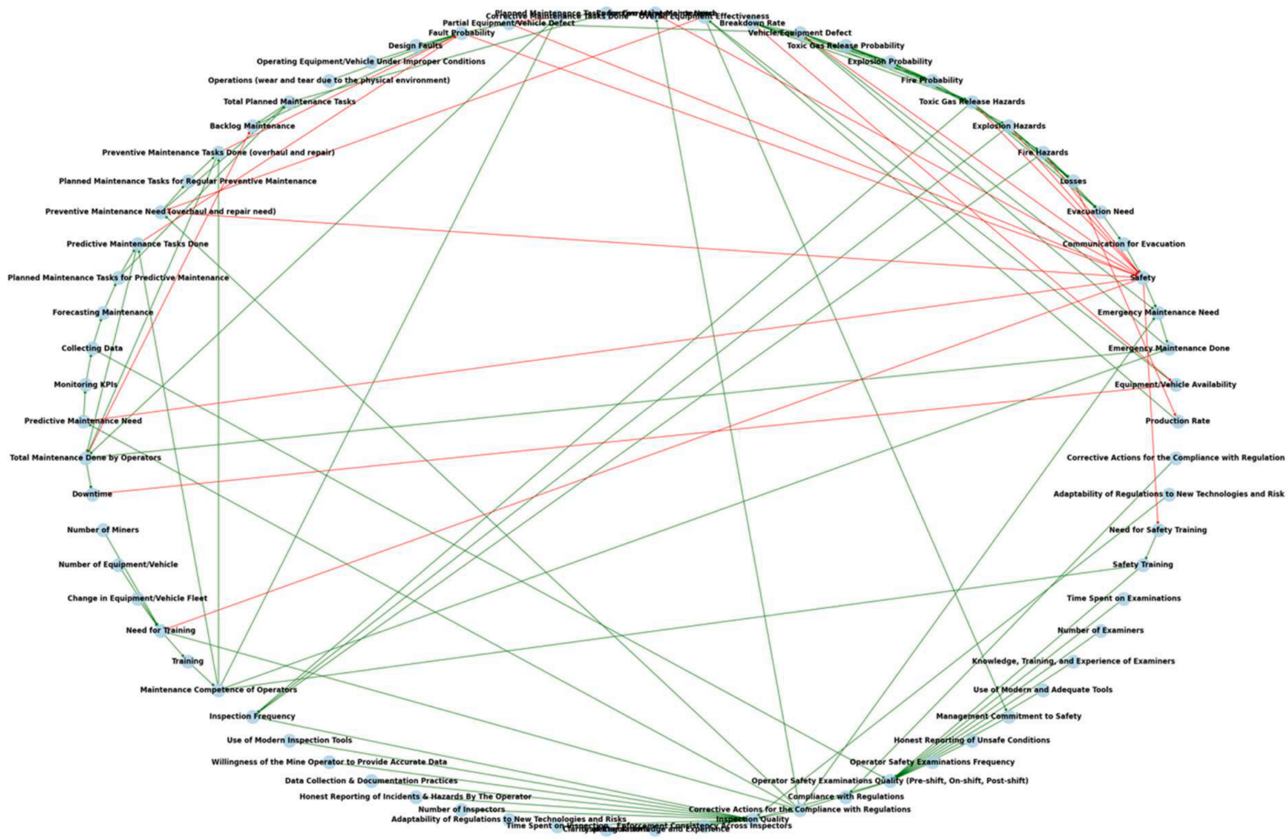

Fig. 4. Network version of CLD.

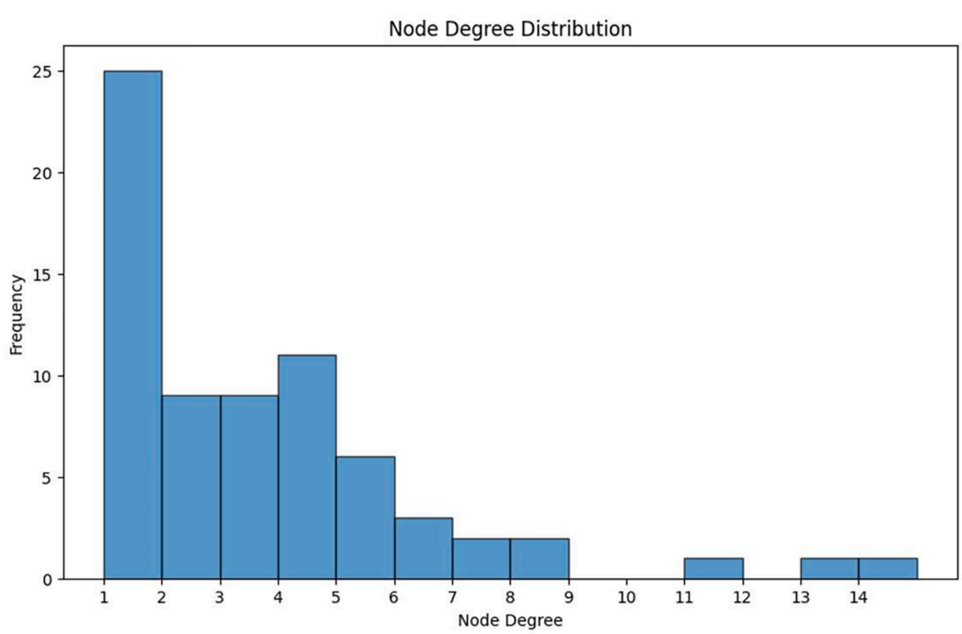

Fig. 5. Node degree analysis result.

most significant subset of nodes, 45 nodes, where each node is reachable from every other within the subset, indicating a tightly interrelated core within the system. The size of the GCC provides insights into system resilience: a larger GCC suggests higher interconnectedness and complexity, making targeted interventions more impactful but also potentially more difficult to isolate.

In addition to node degree, clustering coefficient, community structure, and giant connected component analysis, betweenness centrality was calculated to identify further critical nodes that act as key intermediaries within the system. Betweenness centrality measures how often a node appears on the shortest paths between other nodes, reflecting its importance in maintaining network connectivity and flow

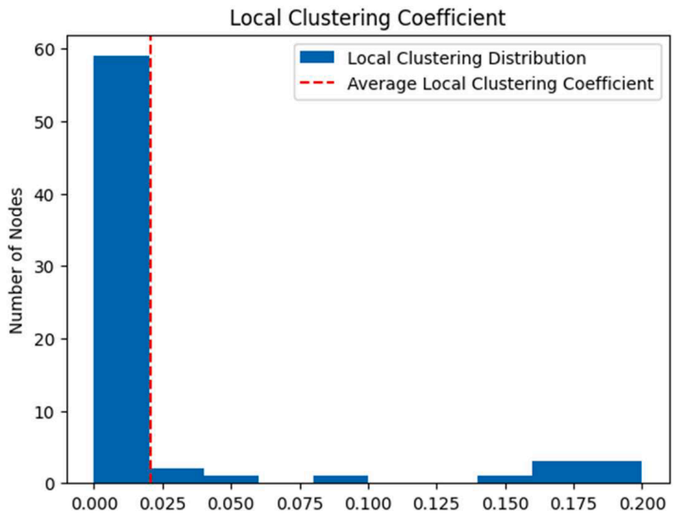

Fig. 6. Local clustering coefficient result.

[36]. The top ten nodes with the highest betweenness centrality values were identified. 'Corrective Actions for the Compliance with Regulations' exhibited the highest betweenness centrality (0.231), followed by 'Vehicle/Equipment Defect' (0.208) and 'Safety' (0.185). Other high-ranking nodes included 'Emergency Maintenance Done', 'Emergency Maintenance Need', 'Fault Probability', and 'Operator Safety Examinations Quality (Pre-shift, On-shift, Post-shift)'. These results highlight the pivotal role of regulatory compliance actions, safety performance, and emergency-related activities in linking different parts of the system, serving as structural bridges between otherwise less connected subsystems.

To assess the system's resilience and vulnerability, that is, its ability to maintain critical safety and maintenance functions and to identify weak points that could amplify BEV fire-related disruptions, a targeted attack simulation was conducted by removing the top five nodes with the highest betweenness centrality: 'Corrective Actions for the Compliance with Regulations', 'Vehicle/Equipment Defect', 'Safety', 'Emergency Maintenance Done', and 'Emergency Maintenance Need'. After removing these critical nodes, the size of the giant connected component (GCC) was recalculated. The GCC size dropped significantly from including most nodes in the original network to 63 nodes in weakly connected components and only seven nodes in the largest strongly connected component. This drastic reduction demonstrates that these key nodes are central to maintaining system connectivity and overall structural integrity, indicating that disruptions to these elements could fragment the interactions among operational, safety, and regulatory processes that are critical for preventing and managing BEV fire events.

Supporting this observation, the network density, a measure that shows how connected a network is, quantifying the ratio of actual connections (edges) in the network to the total possible connections between all nodes, was calculated as approximately 0.024 [38]. This low density indicates a sparsely connected structure where most nodes are linked through a small number of key pathways rather than densely interconnected clusters. The combination of a high GCC size with low density suggests that while the system appears cohesive under normal conditions, it is structurally vulnerable to disconnection if critical nodes or links are removed. This characteristic emphasizes the importance of maintaining and protecting central components within the system, particularly those related to regulatory compliance, equipment fault management, and emergency maintenance, to preserve overall system resilience and operational safety.

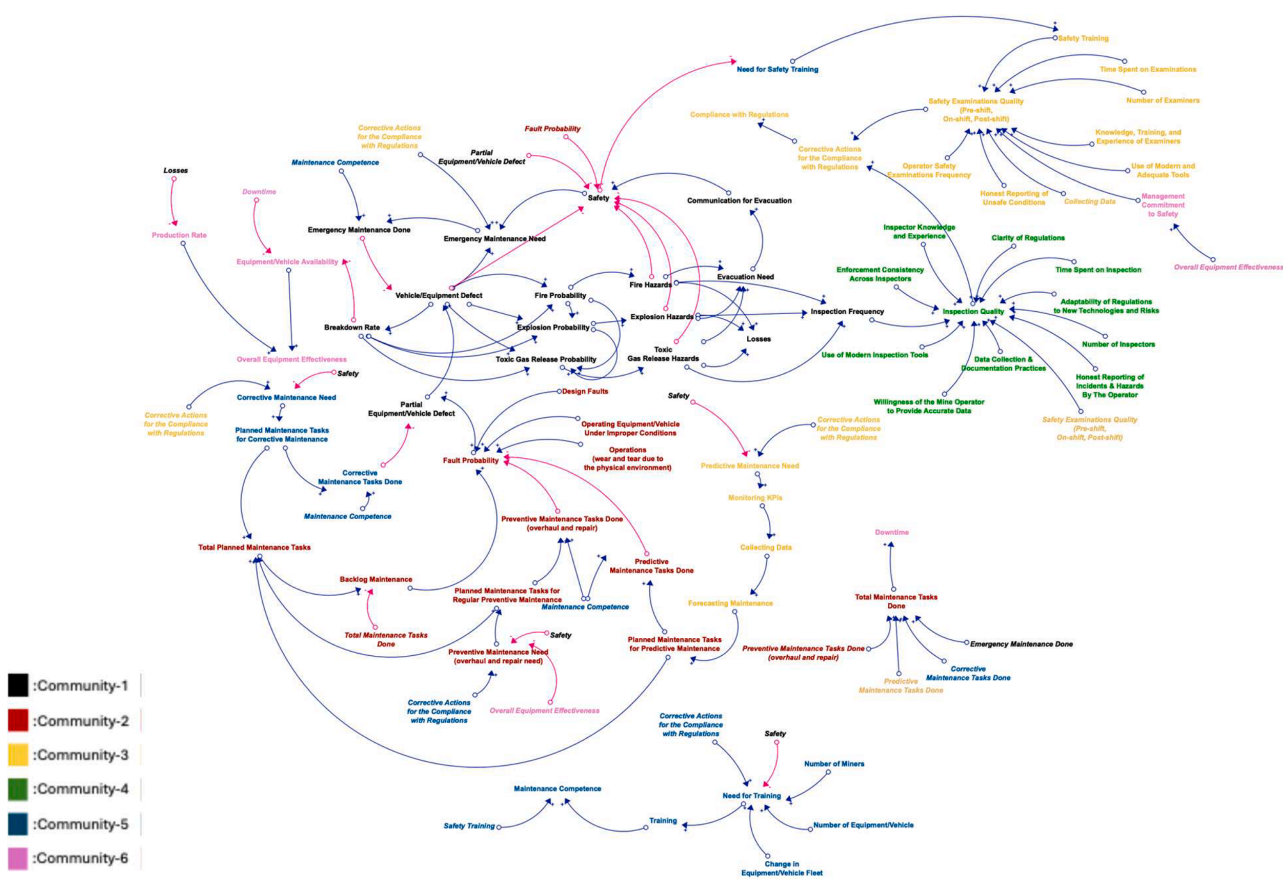

Fig. 7. Communities in CLD.

These findings suggest that specific regulatory, maintenance, and safety-related elements not only directly influence fire risk but also serve as central points that hold the broader safety management system together in TRM operations. Interventions or failures involving these critical nodes would likely have disproportionate effects on system resilience, making them strategic targets for risk mitigation and safety improvement efforts.

3.1.3. Analysis of operational parameters of TRM using HaulSim simulations

HaulSim is a simulation software designed for the mining industry, enabling users to model and analyze haulage routes, equipment performance, and operational constraints. Simulating various scenarios helps identify bottlenecks and improve operational efficiency. However, the effectiveness of HaulSim depends on the accuracy and validity of the models, which must closely represent real-world processes to predict outcomes [12] reliably.

In this study, HaulSim was used to generate input parameters for the SFD, specifically capturing the operational stress imposed on batteries under various conditions and different equipment fleets. These simulations were developed based on the layout and potential equipment fleet of the level where the battery fire occurred at the TRM, reconstructed using information from the literature and the MSHA's incident investigation reports [29,30]. Haulage routes and equipment movements, including those of haul trucks and LHDs, were modeled according to the layout and operating conditions, with two shifts running 22 h per day to reflect realistic operating conditions. The simulated mine layout of the level where the battery fire happened is shown in Fig. 8.

In Fig. 8, the locations of the battery fire and battery swapping station are shown on the mine layout simulated using HaulSim. In this operation, ore and waste are often moved several times before reaching the surface. After being mucked from the production face, Drifts 1, 2, 3 and 4 shown in Fig. 8, the material is first placed in a re-muck bay to maintain cycle efficiency. From there, trucks transport it to material handling drifts (MHDs), where load–haul–dump (LHD) units re-handle and transfer it to the skip loading area. Within the material handling drift, trucks dump material into short drifts, and loaders then move it to the grizzly, apron feeder, and finally through a short conveyor to the skip loading system for hoisting to the surface [29]. Hence, in HaulSim, it was simulated that the haul trucks work between the drifts and re-muck bays, then they move this material to MHD to be re-handled by LHDs and skip to the loading system. As the exact fleet information was unknown for TRM, various scenarios with different equipment fleets were created based on the experts' recommendations. The scenarios simulated in HaulSim are:

- **Scenario 1:** One BEV (Sandvik Z50 haul truck), three diesel haul trucks (CAT AD30), 8 diesel LHDs (CAT R1600h)
- **Scenario 2:** Two BEVs (Sandvik Z50 haul trucks), two diesel haul trucks (CAT AD30), 8 diesel LHDs (CAT R1600h)
- **Scenario 3:** Three BEVs (Sandvik Z50 haul trucks), one diesel haul truck (CAT AD30), eight diesel LHDs (CAT R1600h)
- **Scenario 4:** Four BEVs (Sandvik Z50 haul trucks), eight Diesel LHDs (CAT R1600h)
- **Scenario 5:** four BEVs (Sandvik Z50 haul trucks), eight electric LHDs (Epiroc's Scooptram ST10 G)

In Scenario 1, a single BEV operates between re-muck bay 4 and MHDs. In Scenario 2, one truck operates between re-muck bay 2 and MHDs, while another operates between re-muck bay 4 and MHDs. Scenario 3 involves three BEVs: the first operates between re-muck bay 1 and MHDs, the second between re-muck bay 2 and MHDs, and the third between re-muck bay 3 and MHDs. In Scenarios 4 and 5, four BEVs are in operation, with the first assigned to re-muck bay 1 and MHDs, the second to re-muck bay 2 and MHDs, the third to re-muck bay 3 and MHDs, and the fourth to re-muck bay 4 and MHDs.

Although it was known that only Sandvik's Z50 haul trucks were used at TRM as BEV, Scenario 5 was created to analyze how the temperature and battery fire probability would change if the entire equipment fleet were electric, using Epiroc's Scooptram ST10G electric LHDs. Epiroc's Scooptram ST10G electric LHD is selected for Scenario 5 because it has the same capacity as the CAT R1600H. Since the Sandvik Z50 haul truck and Epiroc's Scooptram ST10G electric LHDs, used in the scenarios, use a battery swapping system, the number and conditions of swapping events were considered as key operational variables in the analysis. The outputs from HaulSim that were incorporated into the SFD include CT, daily CC, BSF per day, and the energy level before swapping, which indicates the DoD for each battery. Because in TRM case, it was known that the fire happened in Z50 haul truck's battery.

The average CT outputs from HaulSim for Sandvik's Z50 BEV haul

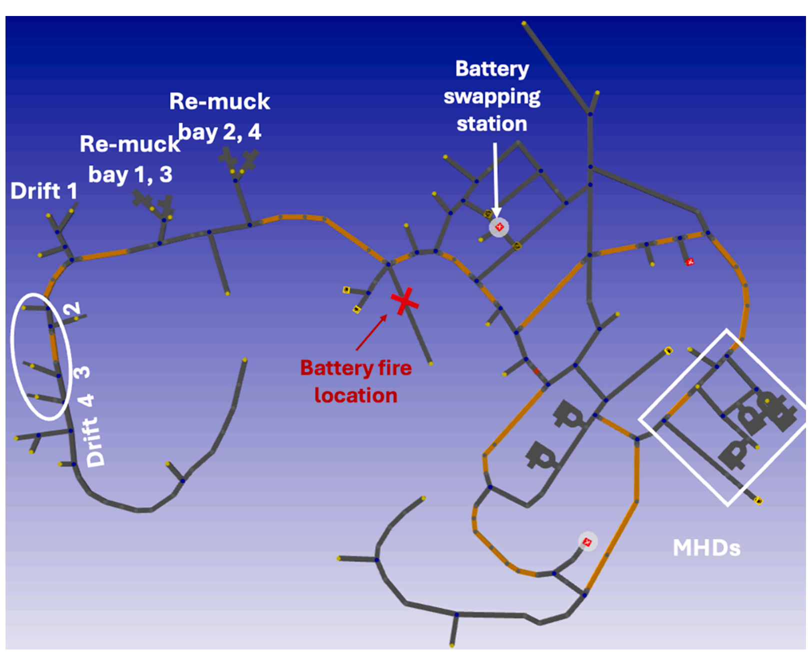

Fig. 8. The level of the TRM layout where battery fire happened.

trucks in each scenario, along with their standard deviations, are presented in Table 1, with the standard deviations corresponding to the re-muck bays where the trucks are working.

As shown in Table 1, the haul trucks operating between re-muck bay 4 and MHDs exhibit the highest CT due to the long distance between drift 4 and re-muck bay 4, whereas those operating between re-muck bay 1 and MHDs have the lowest CT due to the short distance between drift 1 and re-muck bay 1, as loading is an essential factor of total CT. For all equipment, the minimum and maximum CT are 13 min and 40 min, respectively, according to the HaulSim results.

The DoD outputs of Sandvik's Z50 BEV haul trucks in each scenario were calculated according to the energy levels (%) before battery swapping outputs of HaulSim with the equation below:

$$DoD = 1 - EL$$

where DoD is depth of discharge, and EL is energy level (%) data from HaulSim. According to this calculation, average DoD values and standard deviations for each BEV in each scenario are shown in Table 2.

The high DoD values in Table 2, higher than 0.80, show high potential of electric short circuits and fast aging in batteries [39]. The minimum and maximum DoD values are 0.00 and 0.99, respectively, according to the HaulSim results.

The number of battery swaps and CCs per day outputs for Sandvik's Z50 BEV haul trucks in each scenario is shown in Table 3.

Since the simulations were conducted daily, single values were found and shown in Table 3 for the number of battery swaps and CCs per day for each BEV.

The outputs generated by HaulSim and shown in Tables 1–3, including CT, DoD, daily CC, and BSF, provide critical insights into the operational stresses experienced by the battery systems of electric vehicles. These parameters serve as indicators of the evolving likelihood of different types of faults that can lead to thermal runaway and fire events. For instance, frequent deep discharges may increase the risk of electrical shorts, while extended CT can indicate potential traffic congestion underground, which raises the likelihood of vehicle collisions and associated mechanical damage. Similarly, a higher BSF may reflect increased handling frequency, elevating the probability of mishandling or impact-related faults. Operational stresses can also occur during the swapping process itself, whereas charging events may raise battery temperatures, particularly in areas with insufficient ventilation, potentially accelerating aging processes or triggering thermal abuse conditions. By analyzing the distributions of these operational parameters, this study uses them as inputs in a SFD to evaluate how the probabilities of these fault conditions evolve under different scenarios. In this way, the simulation results from HaulSim are transformed into dynamic representations of how operational practices influence battery stress and fire risk over time.

3.1.4. Analysis of underground environmental parameters of TRM using VentSim simulations

VentSim is a simulation software used for the mining industry that allows users to model and evaluate ventilation systems, including airflow, heat transfer, contaminant dispersion, and associated costs. It provides a comprehensive and integrated platform for designing and optimizing mine ventilation networks [13].

VentSim was used to simulate the wet bulb global temperature (WBGT) of the TRM because it is another factor that may trigger the increase of the cell temperature of the lithium-ion battery and lead to lithium-ion battery fires [40,8]. As a result, five scenarios introduced in the HaulSim simulations were simulated in VentSim to investigate how WBGT in TRM changes with varying equipment fleets utilizing the mine layout and the airflows shown in the MSHA reports [30]. The results of these simulations for each scenario are presented in Figs. 9–13.

Figs. 9–13 illustrate the ambient temperature values for the considered scenarios based on the TRM layout, in wet bulb globe temperature (WBGT) units. The WBGT values less than or 24°C are shown in green, WBGT values between 24°C and 26°C are shown in yellow, and WBGT values higher than 26°C are shown in red in these results. According to the results, the temperature of the underground mine increases as the number of diesel vehicles in the equipment fleet increases. Since the heat emission efficiency BEVs are three times higher than diesel vehicles [41].

For each minute of operation during a typical workday in the mine, temperature data were extracted at two critical points: one where a battery fire occurred and another where battery swapping is performed. The first location was selected because a battery fire was observed there, and according to the results, it represents one of the hottest areas along the paths traversed by the battery. The second location, where battery swapping occurs, was chosen because its temperature is also crucial; as the depleted battery is being recharged, it is already warm, and proper ventilation at this site is essential to prevent overheating. Elevated temperatures accelerate exothermic reactions within LIBs, causing the solid electrolyte interphase (SEI) to collapse, separators to melt, and electrodes to short-circuit, which significantly raises the likelihood of cell aging and thermal runaway beyond 25°C [8]. Even a temperature rise of 10°C above this threshold can double the degradation rate of lithium-ion battery components, making thermal management critical for safe operation [42]. Additionally, work environments with a WBGT above 26°C are considered "hot" sites by MSHA due to increased thermal stress and accident risk, and operations above this limit are generally not permitted [43]. In this study, 26°C WBGT was defined as the critical temperature threshold for the TRM. Temperatures above this level were examined, as the upper limit of the optimal operating range for the LFP batteries used in this case is 45°C, corresponding to approximately 31.5°C WBGT under underground conditions according to VentSim simulations [44]. For these reasons, the temperature values at the two selected points served as another inputs for the SFD.

3.1.5. Stock-flow diagram (SFD)

A SFD diagram in SDM is a way to represent how systems change over time using a set of basic building blocks. These building blocks are shown Fig. 14.

As shown in Fig. 14, stocks, also called levels, are accumulations that represent the current state of something, whether concrete, like a population or water behind a dam, or abstract, like happiness or fear. These can also be modeled as conveyors when there is a time delay before the stock changes, such as seedlings maturing into trees. Flows, shown as pipelines with valves in Fig. 14, represent the activities that increase or

Table 1
Average CT and standard deviations of BEVs.

	Re-muck Bay 1		Re-muck Bay 2		Re-muck Bay 3		Re-muck Bay 4	
	Average CT (min)	Standard Deviation	Average CT (min)	Standard Deviation	Average CT (min)	Standard Deviation	Average CT (min)	Standard Deviation
Scenario 1	-	-	-	-	-	-	25.14	1.03
Scenario 2	-	-	23.79	2.90	-	-	25.09	1.03
Scenario 3	18.99	4.41	22.15	3.06	20.00	4.60	-	-
Scenario 4	19.00	4.22	22.01	3.03	19.55	4.71	24.78	1.86
Scenario 5	17.85	2.00	27.68	2.00	24.60	3.00	31.10	2.00

Table 2
Averages and standard deviations of DoD values.

	Re-muck Bay 1		Re-muck Bay 2		Re-muck Bay 3		Re-muck Bay 4	
	Average DoD	Standard Deviation	Average DoD	Standard Deviation	Average DoD	Standard Deviation	Average DoD	Standard Deviation
Scenario 1	-	-		-	-	-	0.90	1.57
Scenario 2	-	-	0.90	1.59	-	-	0.88	2.06
Scenario 3	0.94	0.82	0.88	2.27	0.99	1.15	-	-
Scenario 4	0.94	0.57	0.87	1.11	0.99	1.19	0.90	0.93
Scenario 5	0.96	1.40	0.90	1.65	0.85	2.25	0.91	1.28

Table 3
BSF and CC Per Day of BEVs.

	Re-muck Bay 1		Re-muck Bay 2		Re-muck Bay 3		Re-muck Bay 4	
	BSF per Day	CCs per Day	BSF per Day	CCs per Day	BSF per Day	CCs per Day	BSF per Day	CCs per Day
Scenario 1	-	-	-	-	-	-	12	44
Scenario 2	-	-	13	46	-	-	12	44
Scenario 3	15	58	13	51	14	54	-	-
Scenario 4	15	58	13	51	14	54	13	50
Scenario 5	16	60	11	42	15	45	10	38

decrease stocks, such as birth rates, cash flow, or emissions. They act as control variables that drive changes in the system. Clouds are used to represent sources or sinks that lie outside the system boundary. Converters transform or transfer information between parts of the system, sometimes acting like stocks themselves when no flows are present and may include time-dependent or functional relationships. Finally, connectors show the causal links between elements, indicating how information and actions move from one variable to another [25].

To quantify the lithium-ion battery fire risk change with time according to the scenarios simulated in HaulSim and VentSim for the TRM case, SFD was created in Stella using these building blocks. The parameters used in the SFD were derived from a combination of regulatory investigation reports, open-source technical documentation, expert judgment, and physics-based simulations. Table 4 summarizes the data sources and corresponding parameters used for model parameterization.

As summarized in Table 4, MSHA reports were used to reconstruct incident conditions, while BEV specifications and operational assumptions were obtained from manufacturer documentation and published literature. Where site-specific data were unavailable, expert interviews informed representative operating practices. Time-dependent operational and environmental inputs were generated using HaulSim and VentSim simulations calibrated to the TRM layout.

These SFDs created for each scenario are shown in Figs. 15–19.

SFDs to calculate lithium-ion battery fire probabilities in each scenario shown in Figs. 15–19, fed with the inputs created by VentSim and HaulSim simulations. The CT and DoD for each BEVs used in each scenario were generated in Stella according to the best fit distributions to them, generated in HaulSim simulations. In addition, according to the best fit distributions for the temperature values of the battery swapping station and battery fire location generated in VentSim, these values were generated in Stella to find the battery fire probability for each scenario.

For the daily CCs and BSF, because the HaulSim simulation produced only one daily CC and BSF values, using them as a fixed input would not capture the variability that occurs in real operations. Factors such as operator behavior, equipment condition, maintenance events, and changing mine conditions can cause these values to fluctuate. To represent this uncertainty, a uniform distribution was used in these SFDs to generate data, as it is a simple and unbiased choice when detailed data are not available. The single observed values were treated as an approximate mean, and the possible variation ranges were defined as ± 4 cycles and ± 2 swapping around it. This range was selected based on typical day-to-day fluctuations observed in similar underground haulage operations and expert judgment from operational experience, ensuring that the model captures realistic variability without overestimating it.

Then, for each battery in each scenario, fault probabilities that may be caused by mechanical, thermal or electrical abuses were calculated by probabilities of excessive CT, shown with the '*Z50 Cycle Time Effect on Fault Probability*' converter, extreme DoD values before battery swapping, shown with the '*Z50 DoD Effect on Fault Probability*' converter, exposure to the extreme temperatures, shown with the '*Temperature Effect on Fault Probability*' converter, and breakdown probability coming from the manufacturing related the aging, shown with the '*Breakdown Probability*' converter.

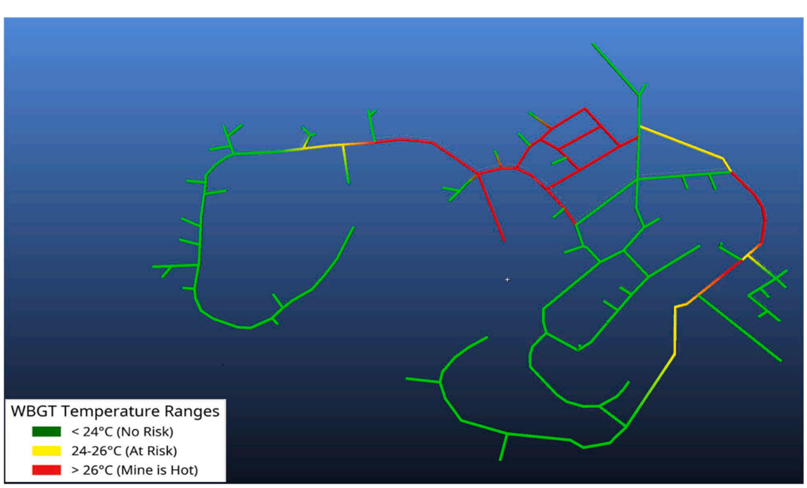

Fig. 9. VentSim results for scenario 1.

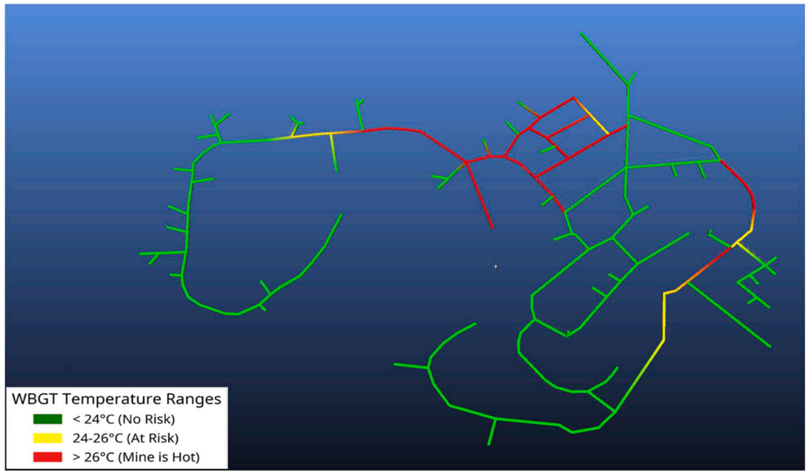

Fig. 10. VentSim results for scenario 2.

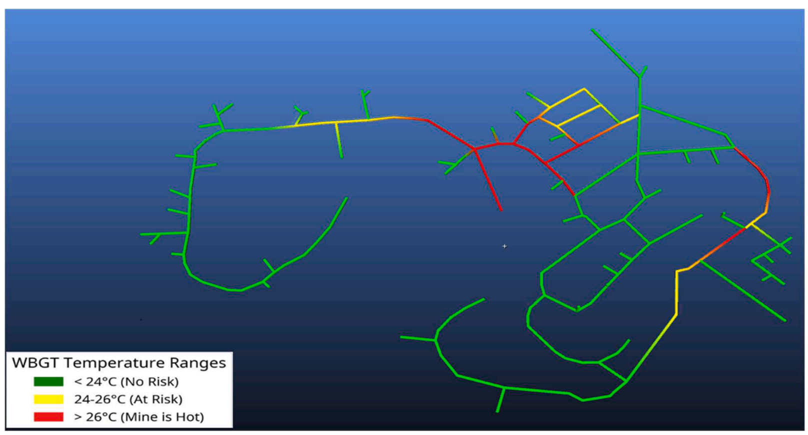

Fig. 11. VentSim results for scenario 3.

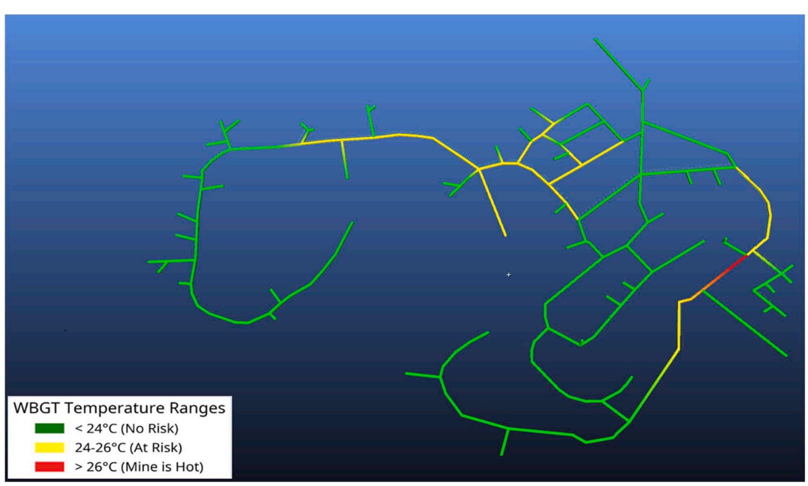

Fig. 12. VentSim results for scenario 4.

The probabilities of excessive CT of BEVs, if the CT is higher than the mean CT, are calculated by the equation below:

$$P(Excessive\ CT) = \frac{\sum (CT - Average\ CT)}{\sum CT}$$

where CT is cycle time data coming from HaulSim. Excessive CT are calculated relative to the average CT for that equipment, because exceeding the average indicates that unexpected conditions have occurred, such as traffic delays, operational interruptions, or prolonged idling. These situations mean the equipment operates longer than expected, which can accelerate battery aging, increase the risk of mechanical damage due to potential vehicle collisions, electrical short circuits, and may lead to higher battery temperatures [45]. The

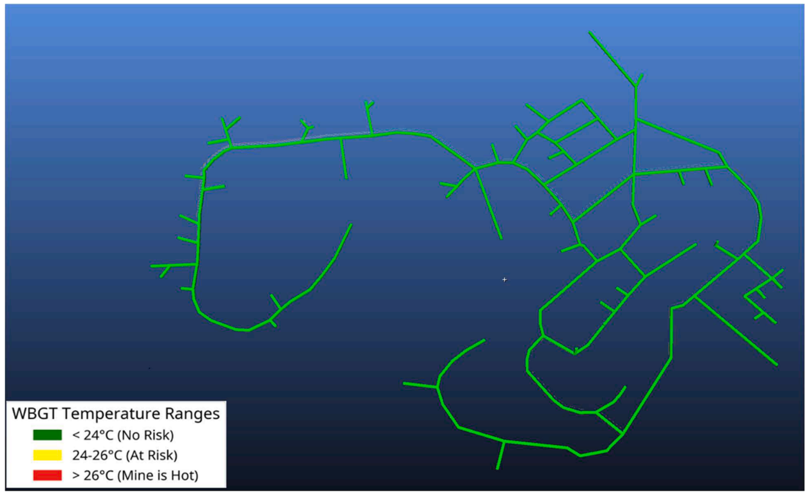

Fig. 13. VentSim results for scenario 5.

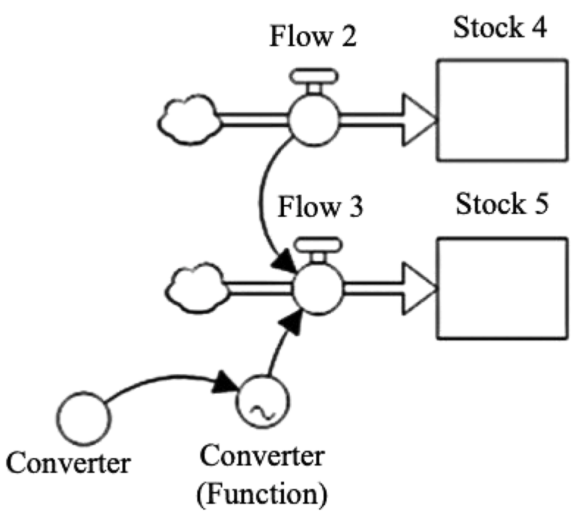

Fig. 14. SFD building blocks [25].

Table 4
Data sources and derived parameters.

Data Source	Extracted / Derived Parameters
MSHA Reports	Safety records, fire case descriptions, maintenance and inspection notes, ventilation conditions, mine layout, fire location, battery swap locations
Open-source technical reports and literature	BEV specifications (battery capacity, chemistry, battery management capabilities), production targets, shift schedules, haulage distances, loading areas, historical BEV fire data
Underground mine expert interviews	Haul distances, fleet composition assumptions, undocumented operational practices
Simulations (HaulSim & VentSim)	Operational and environmental parameters including CT, CC, BSF, DoD, and ambient temperature (WBGT)

approach aligns with time-above-threshold metrics used in reliability engineering to quantify exposure to adverse conditions [46]. Therefore, excessive CT are determined based on deviations from the average CT. The total CT is calculated in Stella by summing the CT generated for each daily cycle, which is also generated within the model. Normalizing by total CT yields a dimensionless probability metric consistent with probability theory fundamentals [47].

The probabilities of extreme DoD values before battery swapping are calculated using equation below:

$$P(Extreme\ DoD) = \frac{N(DoD > 0.80\ or\ DoD < 0.20)}{\sum BSF}$$

where DoD is depth of discharge, and BSF is battery swapping frequency. DoD values are defined based on the DoD immediately before battery swapping. A DoD greater than 0.80 indicates a deep discharge condition, while a value lower than 0.20 suggests a potential overcharging condition [39]. Both conditions are critical factors that can contribute to battery fire risk. Therefore, the probability of extreme DoD is calculated as the ratio of the number of DoD instances above 0.80 or below 0.20 to the total number of DoD measurements, which corresponds to the total number of BSF based on the probability theory fundamentals [47].

To calculate breakdown probability, $P(Breakdown\ Probability)$, of the battery coming from the manufacturing related aging, the Weibull distribution was used from reliability engineering [48]. The Weibull distribution equation is:

$$F(t) = 1 - e^{\left(-\frac{t}{\eta}\right)^{\beta}}$$

where β defines the shape, t defines simulation time, and η defines the scale [48]. In this study, according to [49], saying that Sandvik guarantees that the batteries will maintain at least 60% of their initial capacity over a period of three years, β was selected as 2 and η was selected as 1825.

The probability of each battery being exposed to extreme temperatures is calculated within the SFDs using two approaches. In the first approach, temperature data for every minute in the mine are used to generate daily values in Stella based on a best-fit distribution. The probability is then determined by calculating the fraction of total working minutes during which the temperature exceeds 26 °C WBGT, the critical temperature according to MSHA. In the second approach, the probability is further adjusted by considering how much the temperature exceeds the 26 °C WBGT threshold, resulting in a ratio that reflects the intensity of exposure. The fire probabilities obtained using the first approach are referred to as "strict scenarios," while those calculated using the second approach are labeled as "relax scenarios." For the first approach, strict scenarios, the probability to expose to the extreme temperatures for two points where battery fire happened, and battery swapping is done are calculated with the equation below:

$$P(Exposure\ to\ Extreme\ Temperatures) = \frac{N(T > 26^{\circ}C\ WBGT)}{N(T)}$$

where T is temperature data coming from VentSim in $^{\circ}C\ WBGT$ unit. For

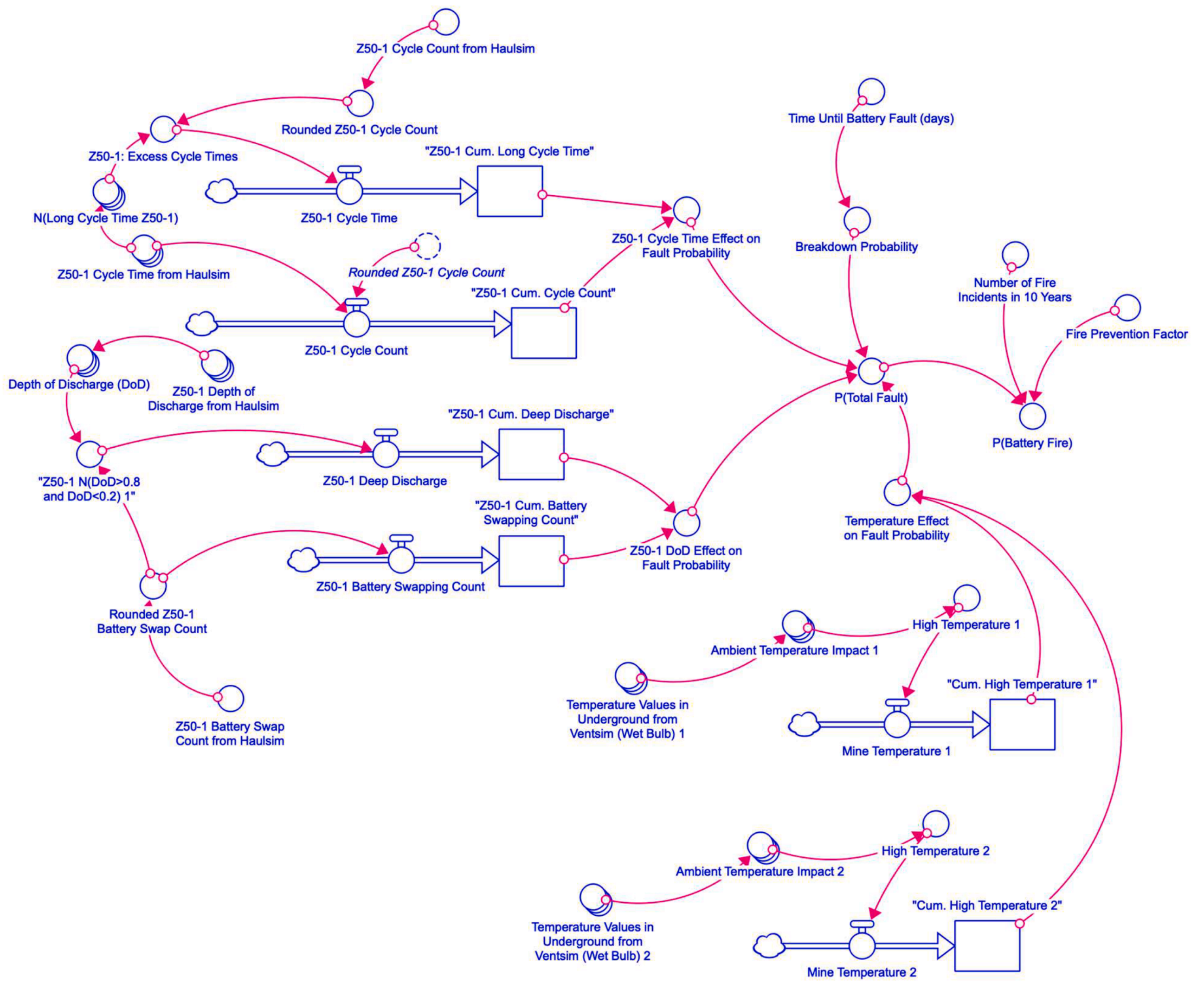

Fig. 15. SFD for Scenario 1.

the second approach, relax scenarios, the probability to expose to the extreme temperatures is calculated with the equation below:

$P(\textit{Exposure to Extreme Temperatures}) = \frac{N(T>26^\circ C\ WBGT)}{N(T)} * \frac{\sum (T-26^\circ C\ WBGT)}{31.5^\circ C-26^\circ C\ WBGT}$ where T is temperature data coming from VentSim in $^\circ C\ WBGT$ unit. In this second approach, if the temperature is higher than 26 °C WBGT, then the ratio that reflects the intensity of exposure, forming the second part of the equation, was added to the equation used in the first approach. 45 °C is the upper limit of the optimal temperature range for the LFP battery which is equal to the 31.5°C WBGT according to the VentSim simulation results for the TRM [44].

As mentioned before at each simulation day, CT, CC, BSF, DoD, and temperature values are regenerated in Stella based on the probability distributions derived from HaulSim and VentSim. Throughout the simulation period, these daily values are accumulated over time, and the probabilities of excessive CT, extreme DoD, and exposure to extreme temperatures are calculated based on the cumulative data, representing the overall likelihood of these conditions occurring during the total simulation time.

The battery fault probabilities for each BEVs are calculated by summing the contributions from probabilities of excessive CT, extreme DoD, breakdown, and exposure to extreme temperatures, with each factor weighted equally, multiplied by 0.25. The battery fault probability is calculated with the equation below:

$$\begin{aligned} P(\textit{Fault})_{Z50_n} &= 0.25 * P(\textit{Excessive CT})_{Z50_n} + 0.25 * P(\textit{Extreme DoD})_{Z50_n} \\ &+ 0.25 * P(\textit{Breakdown Probability}) + 0.25 \\ &* P(\textit{Exposure to Extreme Temperatures}) \end{aligned}$$

where $P(\textit{Fault})_{Z50_n}$ represents the fault probability for battery n (where n=1,2,3,4), corresponding to the Sandvik's Z50s used in the scenarios. Then, the probability of at least one battery fault, shown as $P(\textit{Total Fault})$ in SFDs of each scenario, is calculated by the equation below:

$$P(\textit{Total Fault}) = 1 - \prod_{n=1}^{4} \left[1 - P(\textit{Fault})_{Z50_n}\right]$$

where $n = 1,\ 2,\ 3,\ 4$ represents each individual battery pack ($Z50_n$). After determining the probability of at least one battery fault, the battery fire probability is estimated using the Poisson distribution, applying the thinning theorem, which adjusts the overall event rate (λ) according to the probability of faults leading to fires [50]. Over the past 10 years, four battery fires have been reported in underground mines [2]. In the model, battery fires are assumed to occur whenever battery faults arise, as these faults resulting from human errors, operational stresses, or thermal stresses are considered to trigger the fires. The battery fire probability is calculated with the equation below

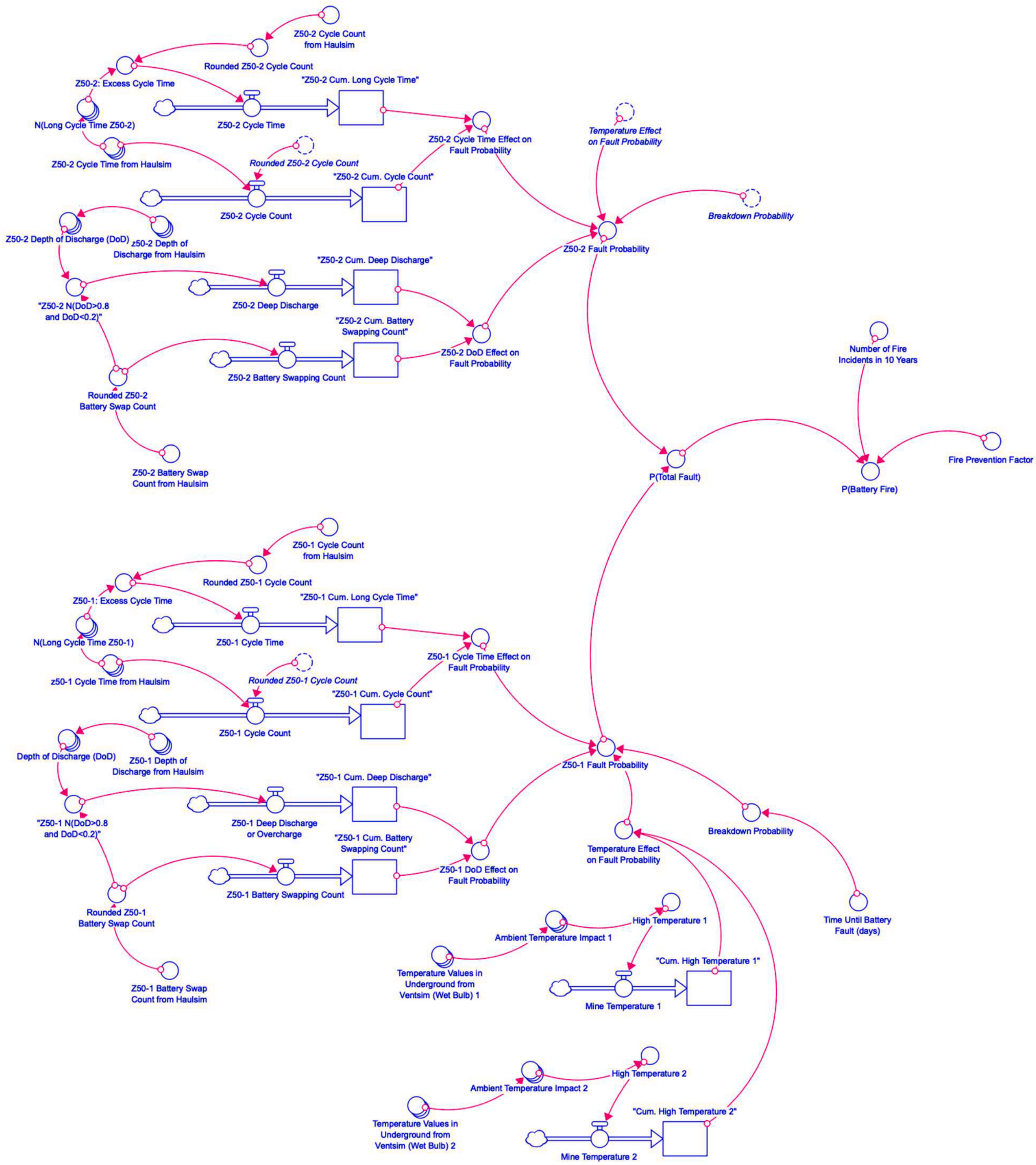

Fig. 16. SFD for Scenario 2.

$$P(Battery\ Fire) = 1 - e^{-\lambda * P(Total\ \ Fault) * t} * (1 - Fire\ Prevention\ Factor)$$

where $\lambda = \frac{4}{365*10}$ per day, and *Fire Prevention Factor* $= 0$ at first, to calculate the fire probability due to the operational and thermal stresses. To evaluate the fire prevention strategies according to the proposed mitigation strategies, this was changed. Results of happening at least one battery fault and battery fire probabilities in a year are provided in Table 5 without considering the fire prevention factor according to the strict and relaxed approaches used to calculate the probability of exposure to the extreme temperatures.

As represented in Table 5, the probability of at least one battery fault follows the order Scenario 4 > Scenario 2 > Scenario 3 > Scenario 5 > Scenario 1 under strict conditions and Scenario 4 > Scenario 5 > Scenario 3 > Scenario 2 > Scenario 1 under relaxed conditions. Although Scenario 1 has the lowest overall fault probability in both approaches, this does not mean it is the safest option. Scenario 1 includes the highest number of diesel-powered equipment, which leads to significantly higher temperature levels in the mine. As a result, the contribution of temperature to the overall battery fault probability is highest in this scenario. This finding indicates that Scenario 1 is not a favorable option for underground operations because one of the main advantages of BEV integration, improved ventilation and reduced heat generation, cannot

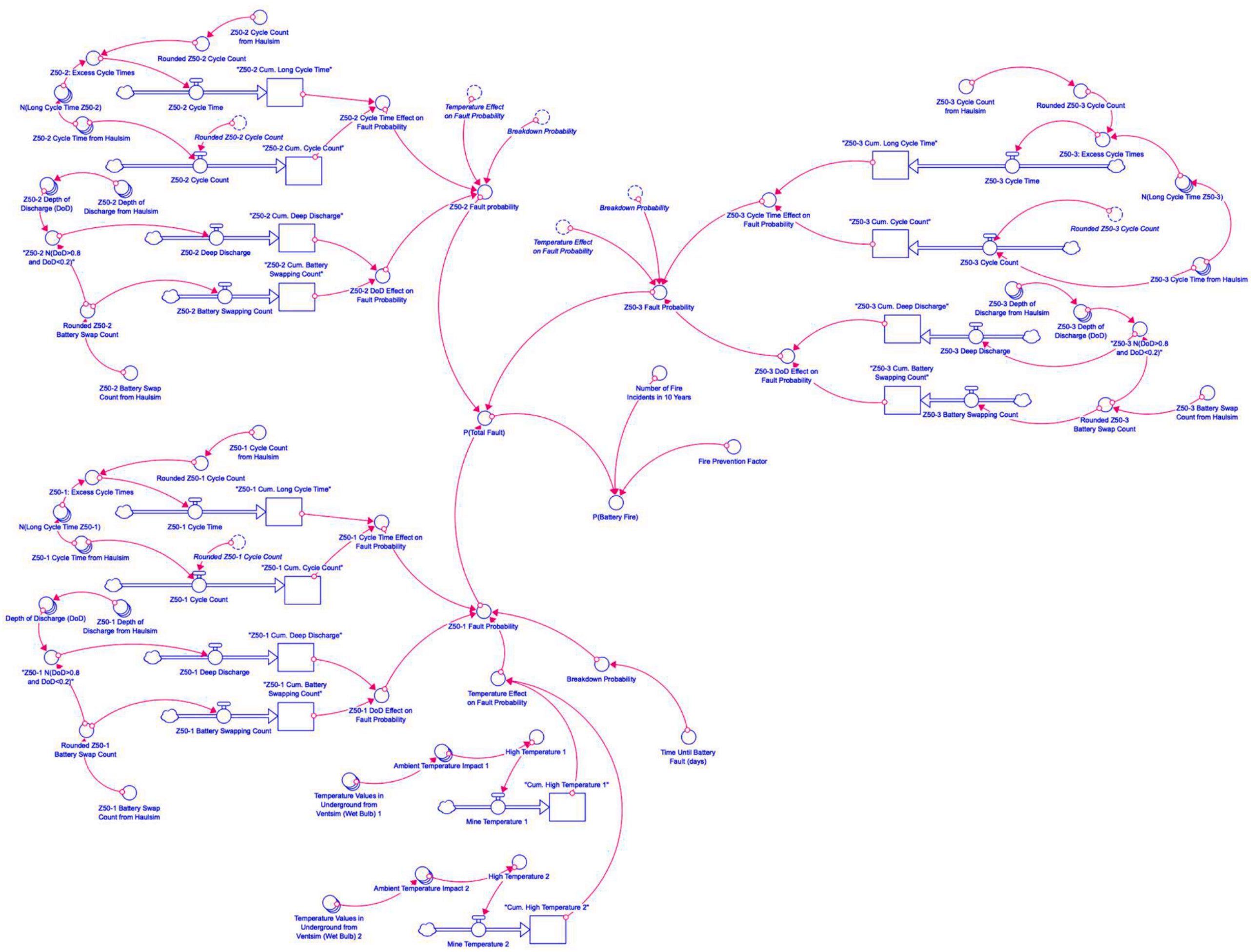

Fig. 17. SFD for Scenario 3.

be realized. The elevated temperature levels suggest that the ventilation system would need substantial improvement to maintain safe operating conditions with the equipment fleet used in Scenario 1.

A comparison between Scenario 2 and Scenario 3 further illustrates the influence of temperature and BEV quantity. Although Scenario 2 shows a higher number of temperature readings above the 26°C WBGT threshold compared to Scenario 3, when the intensity of temperature exposure is considered under relaxed conditions, the temperature-related contribution to fault probability becomes nearly equal in both scenarios. However, because Scenario 3 includes a higher number of BEVs, the overall probability of battery faults is slightly higher.

Under the relaxed approach, the probability of battery faults generally increases as the number of BEVs in the fleet increases, except for Scenario 5. In Scenario 5, temperature values remain well below the threshold, meaning that temperature contributes almost nothing to the fault probability. Under strict conditions, Scenario 4 consistently exhibits the highest fault probability. In this case, as the number of diesel vehicles in the fleet increases, the contribution of temperature to the fault probability also increases, which alters the ranking of both fault and fire probabilities across the scenarios.

3.1.6. Sensitivity analysis for the SFD models. A sensitivity analysis was conducted to evaluate the haulage system's response to production-driven changes, with production rate selected as the primary independent variable. The analysis examined how incremental production increases affect fleet sizing, operational battery parameters, underground thermal conditions, and resulting battery fire probability. Three haulage electrification configurations were evaluated: diesel-powered LHDs with mixed diesel–BEV trucks, diesel-powered LHDs with fully BEV trucks, and fully BEV LHDs and trucks.

Production increases altered the fleet size, battery operating conditions, and underground thermal loads, which were evaluated iteratively using coupled HaulSim operational and VentSim thermal-ventilation simulations.

A summary of fleet composition, operational battery parameters, and thermal responses for all sensitivity cases is provided in Table 6.

Using the BEV parameters summarized in Table 6, the sensitivity of battery fire probability was evaluated using newly developed SDM models. A relaxed approach was used to quantify the effects of temperature on fire probability, and the results were compared with the corresponding base scenarios (Relax Scenarios 1–5).

In the sensitivity analysis of the mixed diesel-BEV truck configuration with diesel LHDs, production increases of 20% and 30% resulted in a clear rise in battery fire probability, as shown in Fig. 20.

As shown in Fig. 20, fire probability increased from 0.10, 0.15, and 0.16 in Relax Scenarios 1–3 to 0.23 and 0.24 under 20% and 30% production increases. While CT, DoD, and BSF remained nearly unchanged, underground temperature rose due to expanded diesel fleets, indicating that fire-risk escalation is driven primarily by thermal stress rather than battery operating conditions.

For the configuration consisting of fully BEV trucks and diesel-powered LHDs, sensitivity analysis showed a pronounced increase in fire probability from 0.216 to 0.302 and 0.322 respectively as production rose by 20% and 30%, as shown in Fig. 21.

As shown in Fig. 21, fire probability increased alongside a substantial CT rise of nearly 10 min due to traffic congestion and waiting delays,

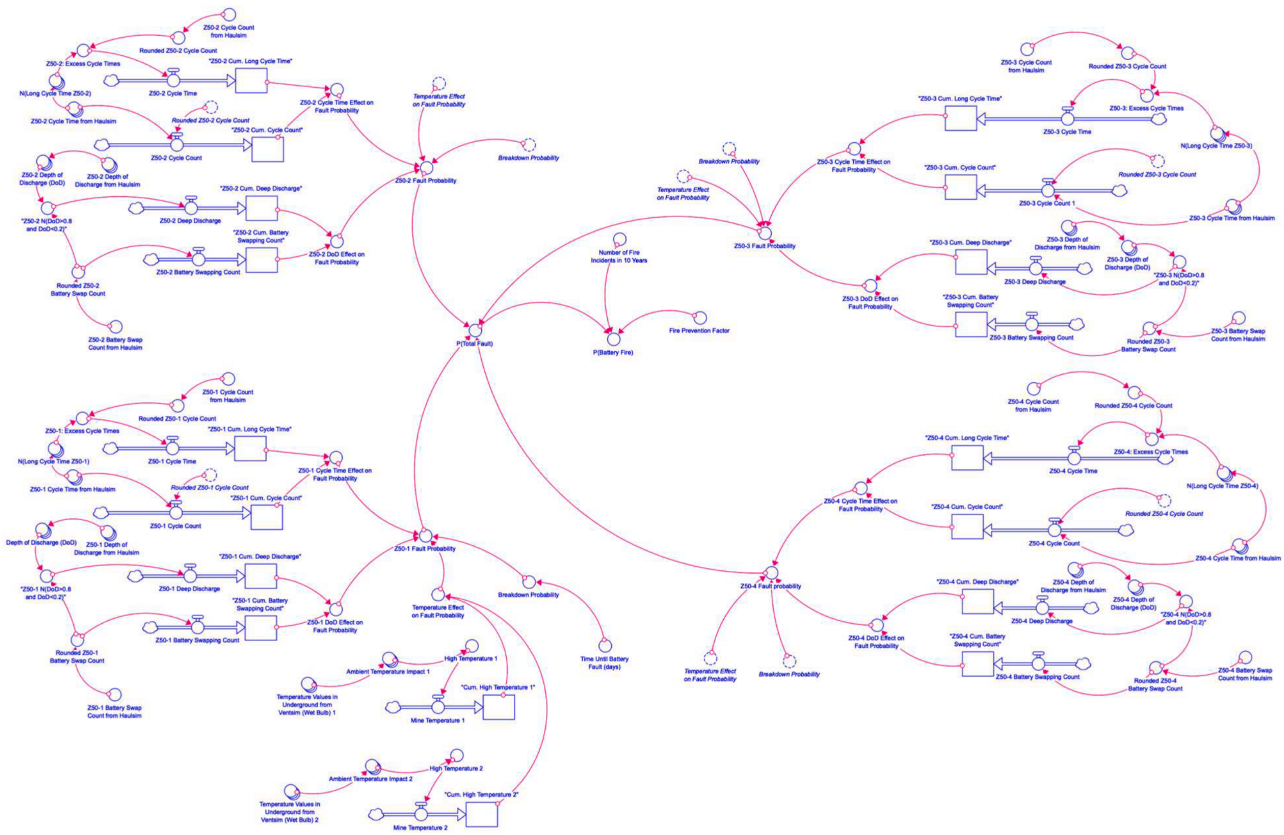

Fig. 18. SFD for Scenario 4.

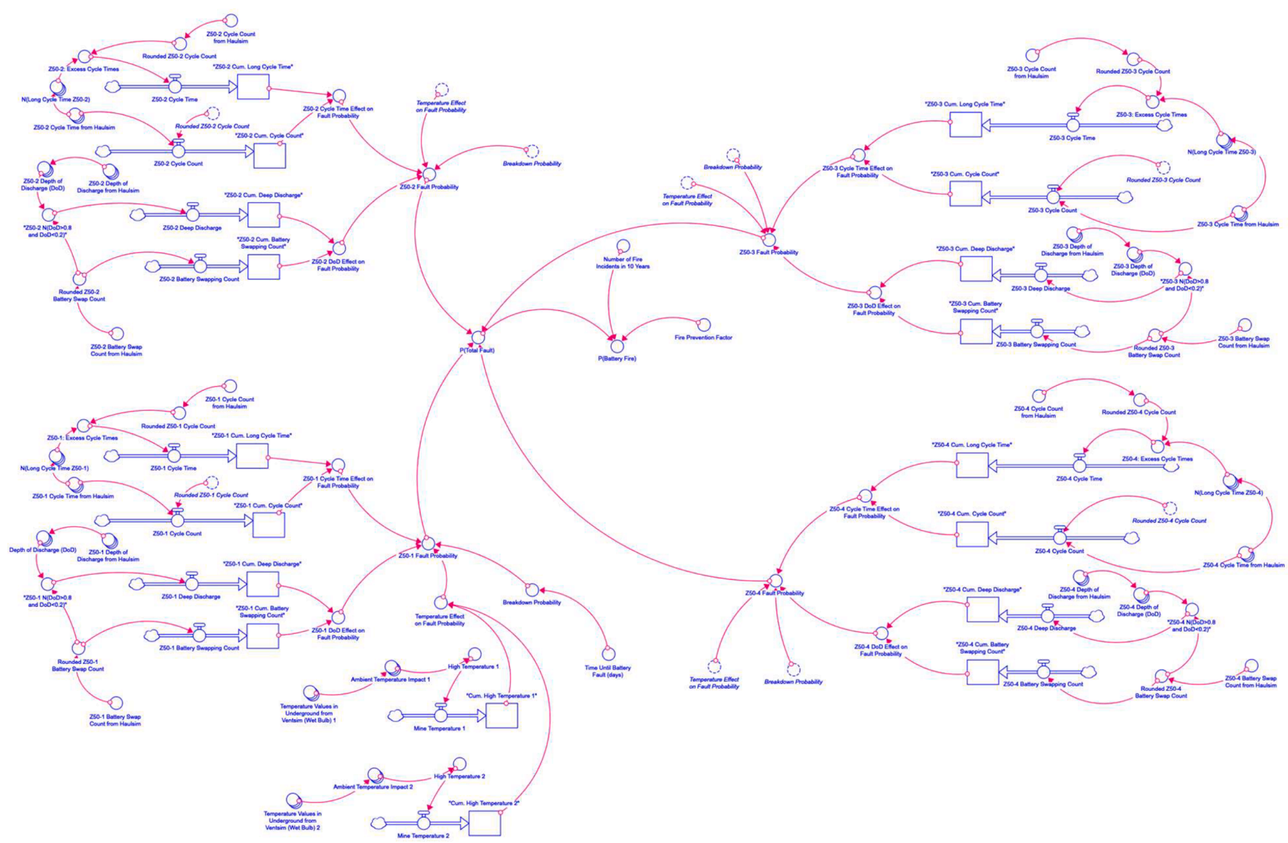

Fig. 19. SFD for Scenario 5.

Table 5
Battery fault and fire probabilities in a year.

	P(Total Fault)	P(Battery Fire)
Strict Scenario 1	0.41	0.15
Relax Scenario 1	0.27	0.10
Strict Scenario 2	0.63	0.22
Relax Scenario 2	0.41	0.15
Strict Scenario 3	0.59	0.21
Relax Scenario 3	0.43	0.16
Strict Scenario 4	0.84	0.29
Relax Scenario 4	0.61	0.22
Strict Scenario 5	0.48	0.18
Relax Scenario 5	0.48	0.18

accompanied by rising underground temperature from diesel heat emissions. Increased traffic density also increases collision risk, raising the likelihood of mechanical battery impact and subsequent fire. Together, these thermal and congestion-driven mechanisms significantly increase fire risk under uncontrolled production expansion.

In the fully battery-electric haulage configuration, the base-case fire probability of 0.18 increased to 0.249 with a 15% production increase, remained nearly unchanged at 30%, and rose to 0.283 at 42% production increase, as shown in Fig. 22.

As shown in Fig. 22, fire probability increased without significant temperature escalation, as diesel heat sources were eliminated. Longer CT resulted from traffic congestion and fixed battery-swapping infrastructure, increasing waiting times. Despite this operational stress, fire-risk growth remained markedly lower than in BEV trucks only scenarios, indicating weaker sensitivity to CT, swapping frequency, and DoD than to ambient temperature.

Collectively, the sensitivity analysis shows that the battery fire risk is most sensitive to environmental temperature and weakly sensitive to operational parameters (CT, DoD, BSF). Diesel fleet expansion drives the strongest thermal risk escalation. In contrast, full fleet electrification significantly weakens thermal-fire coupling, and with effective traffic management through mine layout modifications, dimensional upgrades, or increased swapping capacity, production can be increased while maintaining stable, or even reduced, fire risk.

3.2. Development of the fire prevention strategies

Based on findings from the CLDs and SFDs constructed following the battery fire incident at the TRM, several fire prevention strategies were developed. To provide a quantitative basis for evaluating these strategies, a fire probability model (FPM) was established to quantitatively assess the influence of operational, environmental, and battery-related parameters on battery fire risk.

The FPM integrates regression-based machine learning models through a weighted ensemble (fused model) approach to estimate fire probability across different operational scenarios. This quantitative model enables analysis of how variations in critical parameters, such as temperature, DoD, production rate, and equipment utilization, influence

Table 6
Operational and thermal BEV parameters for sensitivity analysis scenarios.

Scenario	Production Increase	Fleet Composition	Average CT Range (min)	CC Range	BSF Range	Average WBGT (°C)
Mixed diesel-BEV	+20%	10 Diesel LHD, 6 trucks (2 BEV)	27–28	38–40	11–12	33.7
Mixed diesel-BEV	+30%	11 Diesel LHD, 7 trucks (2 BEV)	27–28	38–40	11–12	36.6
BEV Trucks Only	+20%	10 Diesel LHD, 6 BEV trucks	25–34	26–49	8–13	29.5
BEV Trucks Only	+30%	11 Diesel LHD, 7 BEV trucks	24–34	26–44	8–13	30.8
Full BEV	+15%	8 BEV LHD, 5 BEV trucks	24–34	29–48	9–14	16.9
Full BEV	+20%	9 BEV LHD, 5 BEV trucks	19–27	40–67	12–17	17.0
Full BEV	+30%	9 BEV LHD, 10 BEV trucks	26–37	19–30	5–10	17.8

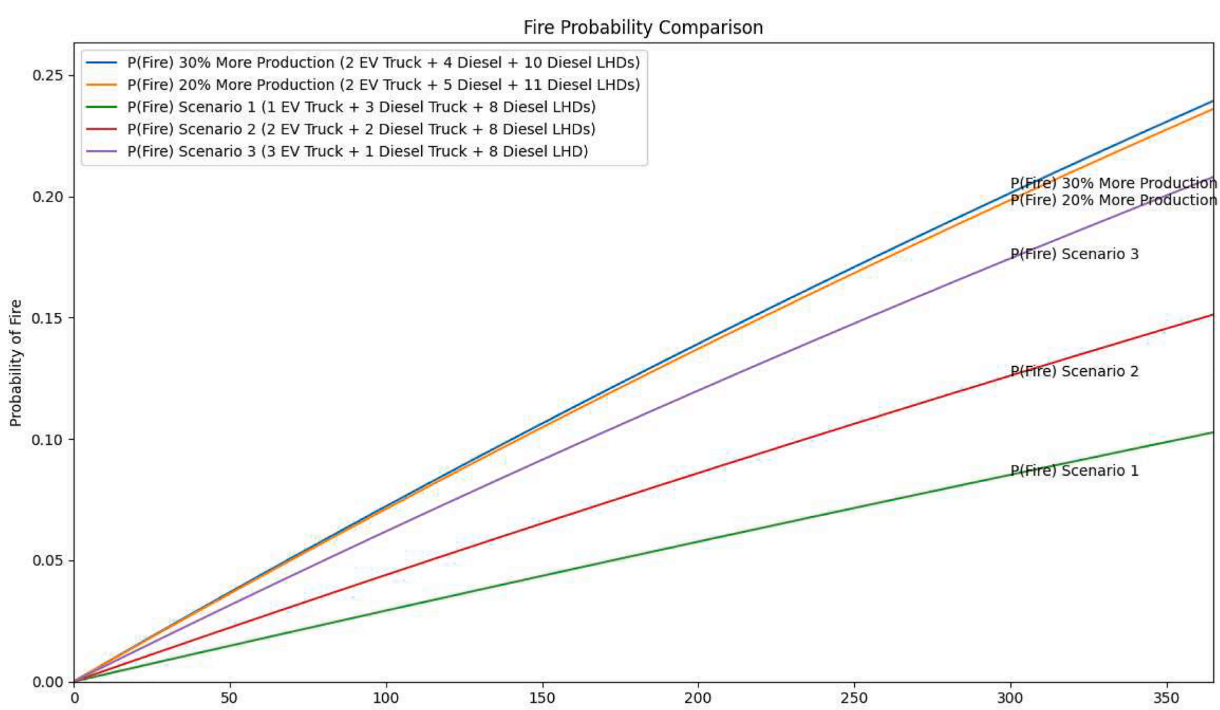

Fig. 20. Fire probability comparison graph for mixed BEV-diesel and base scenarios.

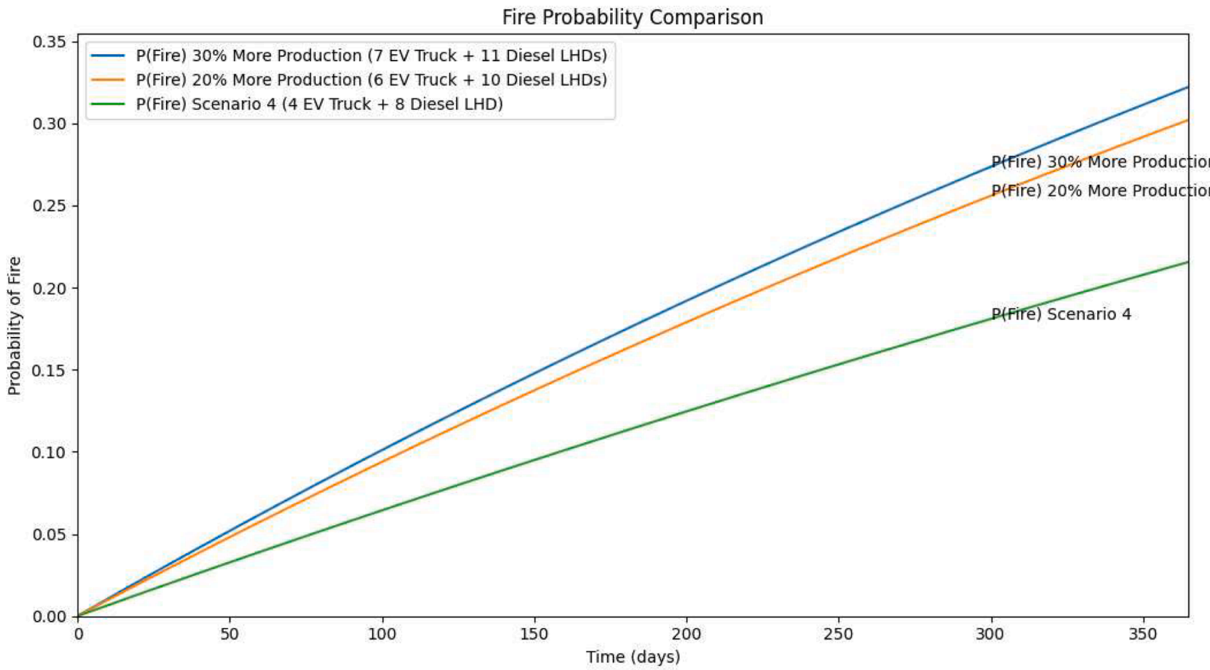

Fig. 21. Fire probability comparison graph for BEV trucks only and base scenarios.

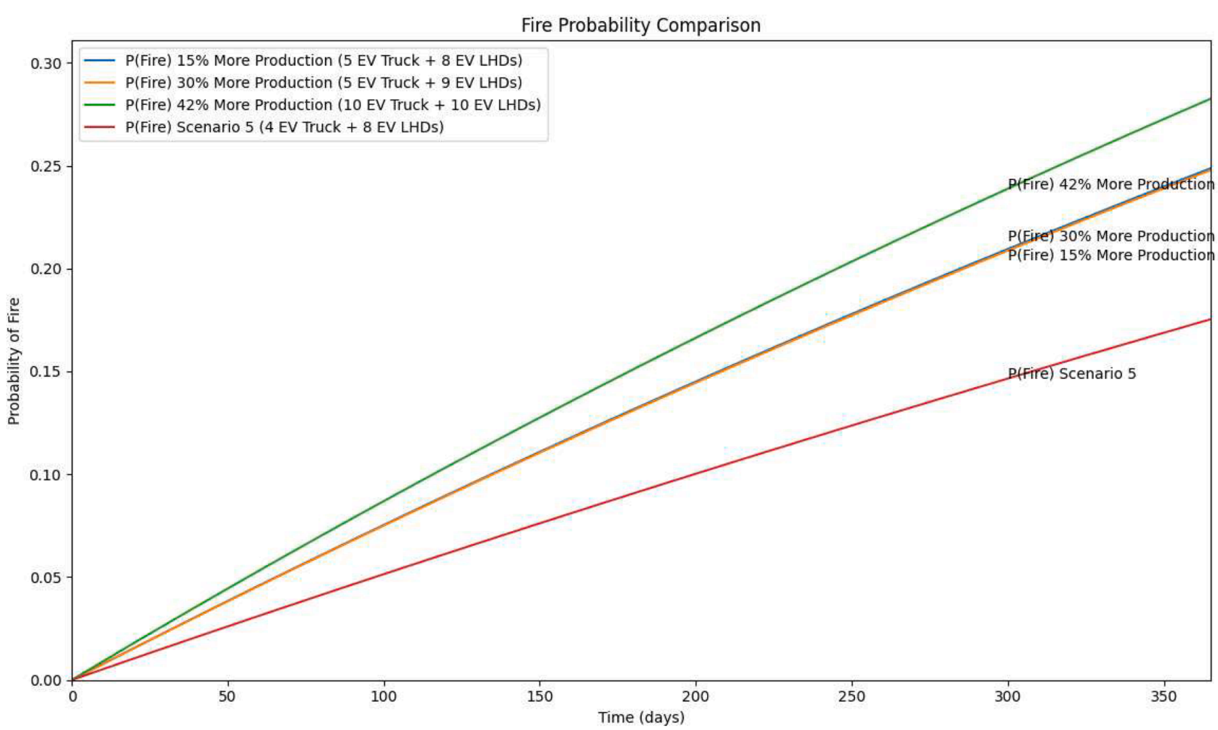

Fig. 22. Fire probability comparison graph for full BEV and base scenarios.

fire risk.

The results from this quantitative framework are subsequently used to evaluate the effectiveness of different fire prevention strategies derived from the CLD and SFD structures. The proposed strategies and their corresponding impacts on the fire prevention factor are illustrated in the SFD and discussed in the following sections.

3.2.1. *Fire probability model (FPM)*

The FPM uses multiple predictor variables representing operational, environmental, and battery-related conditions that influence battery fire risk in underground mining operations. These predictors were derived from the outputs of the SDM, HaulSim, and VentSim simulations developed for the TRM case study. The operational predictors include production rate, number of BEVs, number of diesel-powered vehicles, average CT, and average CC, representing the operational workload and equipment utilization within the mining system. Environmental conditions are represented by the average ambient temperature experienced by the equipment during operation, as elevated temperatures are known to increase the likelihood of battery degradation and thermal instability. Battery-related predictors include the average DoD and BSF, both of which influence battery stress and degradation. Higher DoD values indicate deeper discharge cycles, which can accelerate battery wear and increase the probability of abnormal operating conditions. Similarly, higher BSF reflects more intensive battery usage and charging cycles.

The response variable in the FPM is the estimated probability of a battery fire (P_{fire}) for each operational scenario. The regression-based machine learning models were trained to estimate P_{fire}, and are Ridge regression, LASSO, Elastic Net (EN), Partial Least Squares (PLS), Principal Component Analysis (PCA)-based regression, Random Forest regression (RF), Gradient Boosting regression (GB), and Gaussian Process regression (GP). The use of multiple models allows for the capture of both linear and nonlinear relationships between predictor variables and P_{fire}

Due to the limited number of simulated scenarios, a Leave-One-Out Cross Validation (LOOCV) procedure was employed to evaluate model performance. In LOOCV, each scenario is iteratively removed from the dataset and used as a test sample while the remaining scenarios are used for training. This approach maximizes the use of the available data while providing an unbiased estimate of predictive performance. Model performance was evaluated using the coefficient of determination (R^2) and root mean square error (RMSE). Only models with significant R^2 values were included in the final fused model.

To improve robustness and predictive stability, given the limited dataset, an ensemble fusion approach was adopted. Predictions from individual models were combined using a weighted averaging scheme, with weights inversely proportional to the cross-validated RMSE. Models with higher predictive accuracy, therefore, contributed more strongly to the final fused prediction. The fused prediction is mathematically defined as:

$$P_{fire}{}^{fused}(X) = \sum_{i}^{M} \omega_i * P_{fire}{}^{(i)}(X)$$

where:

- $P_{fire}{}^{fused}(X)$: Fire probability predicted by the fused model,
- M: Total number of models included in the fused model,
- ω_i: Weight of model i, normalized as the inverse of its LOOCV RMSE, i.e., $\omega_i = \frac{1/RMSE_i}{\sum_j^M RMSE_j}$,
- $P_{fire}{}^{(i)}\ (X)$: Fire probability predicted by model i.

Based on LOOCV results, the weights for the models included in the fused ensemble are:

Gradient Boosting (GB): 0.20
Random Forest (RF): 0.18
LASSO: 0.17
Gaussian Process (GP): 0.16
Elastic Net (EN): 0.15
Ridge: 0.14
Then, the final fused prediction equation is:

$$\begin{aligned} P_{fire}{}^{fused}(X) = {} & 0.20P_{fire}{}^{GB}(X) + 0.18P_{fire}{}^{RF}(X) + 0.17P_{fire}{}^{LASSO}(X) \\ & + 0.186^{GP}(X) + 0.15P_{fire}{}^{EN}(X) + 0.14P_{fire}{}^{Ridge}(X) \end{aligned}$$

The fused model demonstrated strong predictive performance with an R^2 of 0.912 and RMSE of 0.019. Bootstrap resampling was also employed to assess prediction stability, yielding a mean R^2 of 0.758 and a mean RMSE of 0.029, further confirming the reliability of the fused estimates.

To quantify how changes in key battery-related and environmental variables influence fire risk, sensitivity analyses were conducted using the fused model. Baseline operational parameters were set to their average values, while individual variables were varied within the ranges observed in the simulation scenarios. Two factors could be adjusted to control the P_{fire} in this case: ambient temperature and battery DoD. Results indicate that increases in temperature lead to substantial increases in predicted P_{fire}. Across the observed temperature range (17.5°C WBGT – 37.5°C WBGT), the fused model predicts an increase in $P_{fire}$of approximately 17%, depending on the production scenario. Similarly, increasing battery DoD (0.85–0.95) results in a predicted P_{fire} increase of approximately 8%.

These findings quantitatively support the importance of effective battery management and thermal control systems in preventing thermal runaway and battery-related fires in underground mining environments.

3.2.2. Fire prevention strategy 1 (Fire prevention factor = 0.00–0.20)

In this strategy, there are only component-level changes intended to reduce the risk of battery fires by enhancing the battery management and control systems (BMCS). BMCS are of utmost significance in ensuring that lithium-ion batteries are functioning safely and efficiently in underground mining, where equipment is exposed to harsh conditions and ought to use high power. At the component level, improvements target the augmentation of the intrinsic functions of BMCS, which are real-time monitoring, diagnostics, and control as a function of voltage, temperature, and current parameters [8]. These functions enable checking limits for detecting risky operating conditions, state estimation for monitoring state of charge and state of health, and fault diagnostics for diagnosing hazards like overcharge, over-discharge, or internal short circuits. Heating management is another critical function, with the goal of keeping temperature levels within safe ranges and avoiding localized overheating through sophisticated cooling techniques like liquid cooling or phase change materials. The latest developments also stress predictive and diagnostic functions, including sensors to detect mechanical stress and track gas emissions related to early thermal runaway stages [8]. Through these improvements in BMCS functions, improving sensing and diagnostic capabilities, and improving heat management, component-level changes directly lower the likelihood of battery faults resulting in fires [8].

Although these improvements may decrease the battery fault or fire probabilities, even if the battery fault or fire probability is detected earlier, the actions needed to prevent the battery fire may not be taken without having continuous feedback loops within the system.

The effectiveness of these battery management improvements is further supported by the quantitative modeling framework presented in this study. The fused model and subsequent sensitivity analyses demonstrate that key battery-related parameters, DoD, and environmental parameters, ambient temperature of the mine, significantly influence the probability of battery fires. Improvements in DoD monitoring, diagnostics, and thermal management systems directly target these critical parameters. Therefore, enhanced BMCS capabilities can reduce the likelihood of operating conditions that lead to thermal runaway, providing a measurable reduction in predicted fire probability.

3.2.3. Fire prevention strategy 2 (Fire prevention factor = 0.2–0.50)

In strategy 2, in addition to the component level changes proposed in strategy 1, the system level changes that need to be done to take the actions for preventing battery faults after detecting the faults in the battery, with the component level changes before battery fires are involved.

According to the CLD, the feedback loops are analyzed to prevent battery faults that may lead to battery fires. For this purpose, the preventive and predictive maintenance, done before any fault to prevent the fault occurrence in the battery, involves loops that need to be improved in the CLD. For this purpose, predictive and preventive maintenance tasks should be increased based on the data provided by the battery management system (BMS). However, this increase also leads to a rise in planned maintenance tasks and backlog maintenance, which can, in turn, contribute to higher fault probabilities. Therefore, the scheduling mechanisms used in mines need improvement, for example, by prioritizing battery-related issues, to prevent unintended increases in fault probability. Additionally, improving the maintenance competence of underground workers and battery manufacturer personnel through safety and maintenance training is crucial because the maintenance activities are generally conducted by manufacturer companies. Such training should include information on early warning systems, BMS functionality, sensors, battery fault mechanisms that can lead to fires, and signs of potential faults. Raising awareness among miners about these issues not only enhances their response capabilities but also helps maintain the safety of the overall system. Ensuring whole-system safety is essential because it relies on effective communication and coordination among different units, such as maintenance, safety and health, and operations. Moreover, analysis of the SFD shows that DoD and temperature are key factors contributing to battery fault probability. Therefore, the dynamic structure of the system should be incorporated into risk assessments and predictive maintenance strategies conducted by mining or manufacturing companies to improve forecasting and decision-making. In addition to this, continuous communications need to be established between the battery manufacturing companies and mining companies to ensure battery maintenance and miners' knowledge about battery fault, fire mechanisms, and their results.

A trade-off exists between maintenance and operational efficiency, as increased maintenance activities can lead to longer downtimes and reduced OEE, potentially lowering management's commitment to safety. Since OEE is a key performance indicator used to measure how effectively equipment is utilized in production, it combines availability, performance, and quality. Therefore, OEE strongly influences managerial decision-making due to reflecting productivity and profitability directly. When maintenance activities increase to improve safety and reliability, they often lead to longer downtimes and reduced OEE. If this reduction is perceived as a loss in operational efficiency or financial performance, management may become less inclined to support safety initiatives, prioritizing production targets instead. As a result, a decline in OEE can negatively affect management's commitment to safety by shifting attention and resources away from safety-related actions toward short-term productivity goals. However, ensuring the safety of the entire system requires evaluating this trade-off carefully. When comparing the consequences of reduced safety with those of decreased OEE, the cost losses associated with fire incidents far exceed those resulting from lower OEE in the long term. As a result, companies may accept a certain reduction in OEE to safeguard system safety and prevent severe losses associated with battery fires.

3.2.4. Fire prevention strategy 3 (Fire prevention factor = 0.50–0.70)

In addition to strategy 2, if the battery fault probability cannot be reduced through improvements in predictive and preventive maintenance and the associated feedback loops, and the fault progresses into a partial or total vehicle or battery defect, the likelihood of a fire can increase significantly. Therefore, feedback loops related to corrective and emergency maintenance must also be analyzed and improved to address partial or total defect formation effectively. The inclusion and enhancement of these loops are critical because corrective and emergency maintenance aim to mitigate faults that have already occurred. However, their integration has operational implications. Emergency maintenance is typically unplanned and performed immediately, whereas corrective maintenance is scheduled. As a result, the total number of planned maintenance tasks will increase, necessitating further refinement of the maintenance scheduling system beyond the improvements proposed in strategy 2. This enhancement is essential to prevent the accumulation of backlog maintenance tasks, which could again elevate the fault probability.

Moreover, given that corrective and emergency maintenance may require longer intervention times, operational continuity and system availability should be considered. To mitigate the impact of extended downtime on OEE during such maintenance events, spare batteries should be stored on-site, or additional equipment, such as a diesel haul truck, should be available to continue operations while the BEV is being serviced.

3.2.5. Fire prevention strategy 4 (Fire prevention factor = 0.70–0.80)

In strategy 4, in addition to the improvements proposed in strategy 3, system-level enhancements at the managerial level are required to establish continuous feedback loops among different system components within the dynamic nature of the underground mining environment. These improvements are essential to ensure overall system safety. To achieve this, mining companies need to revise their safety policies to incorporate structured reporting and communication mechanisms between the maintenance, safety, and health units of the mining companies and the battery manufacturers. Continuous communication between the manufacturer and the mining company must also be formalized through agreements that clearly define terms for collaboration, including provisions for requesting necessary safety and maintenance training to increase technical knowledge and awareness of the miners related to battery fire risks, accessing battery-related information, monitoring battery health, and involving the manufacturer in maintenance activities.

Within the underground mine, key units such as maintenance, ventilation, and production must report to the safety and health unit of the mining company, which should have communication with the manufacturer company, regarding operational status, environmental conditions, equipment health, and emerging hazards, such as increases in battery fire or fault probabilities identified through SDM. The SDM should be actively used by the safety and health unit, which will collect and evaluate reports from all other units. Based on the results of the dynamic model, the safety and health unit must then communicate necessary actions back to the responsible units. For example, if the temperature exceeds safe limits and ventilation adjustments have not been implemented, if there is an accumulation of maintenance tasks, or if a maintenance activity has been identified as required to prevent battery faults, these findings should be reported back to the relevant units for corrective actions.

Additionally, the reporting mechanisms, communication channels between system components, and the implementation of safety policies should be verified through safety examinations conducted by the mining company itself and inspections conducted by the MSHA. To make this possible, the quality and effectiveness of MSHA inspections and safety examinations must be improved by integrating system dynamics-based risk assessments into these processes. Developing adaptive regulations capable of capturing unsafe conditions in mining systems, particularly those integrating new technologies such as BEVs, enhancing inspectors' knowledge of the new risks introduced by advanced technologies, and emphasizing the importance of systems thinking are essential steps toward increasing the inspections quality for maintaining and strengthening safety within underground mining environments. Similarly, increasing the number of safety examiners, enhancing their awareness of new technology-related risks and the importance of systems thinking, promoting honest reporting, and increasing the frequency of inspections can all contribute to improving the quality of safety examinations.

3.2.6. Fire prevention strategy 5 (Fire prevention factor = 0.80–0.99)

In strategy 5, in addition to the improvements proposed in strategy 4, additional preparedness mechanisms need to be improved to decrease the impacts of the battery fires if they cannot be prevented from happening instantaneously. Since mechanical damage or electrical shorts in batteries can cause fires instantaneously, early detection may not be possible. Therefore, emergency preparedness procedures must be enhanced to address the unique nature of battery fires. This includes detecting and locating fires using smoke and heat detectors, initiating immediate evacuation upon fire detection, and isolating the fire in compartments specifically designed for the battery chemistry in use. These compartments should incorporate fire suppression systems proven to be effective for battery fires, as recommended by recent studies [51].

Such measures ensure the safe evacuation of miners and minimize their exposure to toxic gases released during battery incidents [51,7,52]. Locating the compartments to isolate the fires is a critical point because it needs to be selected according to the locations where battery fire probabilities may be high. For this purpose, before integrating batteries into the mine environments, the fire risk in underground mines needs to be assessed carefully with the SDM to see how it could be changed based on the operational and environmental stress factors. Also, hydrogen fluoride (HF), which is a toxic gas that may be released during or right before battery fires, sampling media needs to be provided to the miners to detect toxic gas and start evacuation earlier than observing the fire [7]. According to these improvements in the emergency preparedness plans, the miners need to be trained to know what to do in any emergencies, read the signs of the detectors, and use HF sampling media. In addition, the safety examinations and MSHA inspections should include checking if these improvements are provided and are up and running frequently in the procedures.

3.3. Evaluation of the fire prevention strategies

The fire prevention strategies proposed in this study are designed to work cumulatively, with each subsequent strategy building upon the previous ones to progressively reduce the probability of battery fires. As shown in the SFD, this cumulative effect is represented by the “Fire Prevention Factor” converter, which multiplies the calculated fire probability by a value corresponding to the level of prevention achieved through the selected strategy. For example, implementing the improvements proposed in Strategy 1, which focus on component-level changes, can reduce the fire probability up to 20%. Expanding these measures through strategy 2 may reduce battery fire probabilities up to 50%. Through strategies 3 and 4, which address corrective maintenance, system-level communication, reporting mechanisms, and organizational safety policies, can further reduce the probability to about 70% and 80% respectively. Finally, incorporating emergency preparedness measures described in strategy 5, such as improved detection and suppression systems, compartmentalization, hydrogen fluoride monitoring, and targeted miner training, can reduce the probability by up to 90%. Although complete elimination of battery fire risk is not possible due to the persistent potential for human error, these strategies demonstrate that a comprehensive, multi-layered prevention framework can substantially mitigate the likelihood and consequences of battery fires. By integrating the Fire Prevention Factor into the SFD and adjusting it based on the strategies implemented, the dynamic impact of each preventive action on fire probability can be quantitatively assessed, offering a powerful decision-support tool for mine safety management. In addition to this, since the interactions within the dynamic mine systems are strengthened to ensure safety by implementing these fire prevention strategies, the additional linkages are constructed between the communities found with graph analytics while analyzing the CLD. These additional linkages increase the system’s resiliency, which means even if one of the components of this underground mine system failed, the safety in the system still could be ensured.

3.4. Identification of best performing strategies for fire prevention

The results of the SFD across the five scenarios demonstrate that the effectiveness of fire prevention strategies depends strongly on the composition of the equipment fleet, particularly the ratio of BEVs to diesel-powered equipment, as well as the associated thermal and operational conditions. The cumulative framework proposed for fire prevention strategies in this study, where each strategy builds upon the previous one, shows how progressively enhancing technical, operational, and managerial components can significantly reduce the probability of battery fires.

In Scenario 1, although the probability of battery faults is the lowest among all cases, the contribution of temperature to fault probability is the highest due to the large number of diesel-powered units. This condition negates one of the primary advantages of BEV integration, which is improved ventilation and reduced heat generation. Therefore, in this scenario, component-level improvements alone (Strategy 1) are insufficient to mitigate fire risks effectively. Instead, system-level interventions targeting ventilation improvements and temperature control, combined with strengthened maintenance feedback loops (Strategies 2 and 3), become essential. Additionally, implementing enhanced reporting mechanisms and continuous communication channels between maintenance, safety, and battery manufacturers (Strategy 4) can help detect and address temperature-related risks more proactively. Finally, introducing emergency preparedness measures, such as compartmentalization and improved suppression systems (Strategy 5), is needed as an additional layer of protection against high-temperature-induced battery fires.

Scenarios 2 and 3, which include a higher number of BEVs compared to Scenario 1, show an increase in battery fault probabilities, primarily due to more frequent deep discharge events, extended CT, and the growing impact of aging-related breakdown probabilities. In these cases, preventive maintenance optimization (Strategy 2) becomes particularly critical to reduce fault occurrence before it escalates into severe failures, while corrective maintenance (Strategy 3) supports fault resolution and helps minimize downtime. Considering the modeled results, the battery fault and fire probability values remain very similar across these two scenarios, indicating that operating equipment with two or three batteries introduces nearly the same level of fire risk. In fact, deploying three batteries in the fleet may even be slightly more advantageous, as the temperature values observed underground are comparable to or lower than those in the two-battery configuration. This suggests that, despite the larger BEV fleet, system-level communication improvements and safety policy enhancements (Strategy 4) are sufficient to keep risks manageable when supported by optimized maintenance practices.

Scenario 4, which relies entirely on BEVs for haulage operations, exhibits the highest battery fault probabilities under both strict and relaxed approaches. As the proportion of BEVs increases, the role of technical and organizational strategies becomes even more critical. In this case, at least up to Strategy 4 must be implemented to achieve a meaningful reduction in fault and fire probabilities. Strengthening BMCS capabilities (Strategy 1), predictive maintenance (Strategy 2), and coordinated corrective actions (Strategy 3) lay the groundwork, but organizational-level interventions and continuous risk communication (Strategy 4 and 5) are indispensable to maintain system safety. Without these higher-level strategies, the system remains highly vulnerable to battery-related incidents regardless of the approach used.

Scenario 5, which includes both BEV haul trucks and BEV LHDs, presents a unique case. Despite the high number of BEVs, temperature contributions to fault probability are minimal, and the overall fire probability is lower than in Scenario 4, indicating that improved ventilation and reduced diesel equipment use create more favorable thermal conditions. However, in this fully electrified system, other types of risks such as frequent deep discharges, longer CT, increased likelihood of internal short circuits, and higher susceptibility to mechanical damage, become dominant factors influencing fault probability. As a result, at least Strategy 4 must be implemented to improve the awareness of miners, inspectors, and maintenance personnel, enabling earlier detection and more effective mitigation of these risks. Moreover, because a fire in this scenario has a higher potential to spread rapidly across interconnected electric equipment, emergency preparedness (Strategy 5) becomes particularly valuable in containing potential incidents and protecting overall system integrity.

Overall, the analysis shows that the best-performing fire prevention strategies are highly scenario-dependent. In diesel-dominant environments like Scenario 1, ventilation improvements and stronger communication mechanisms (Strategies 3 and 4) are essential, whereas in mixed or fully electrified systems (Scenarios 2–5), system-level safety policies and organizational awareness (Strategy 4) become the minimum requirement for maintaining safety. Fully electrified scenarios, especially Scenario 5, further benefit from incorporating emergency preparedness (Strategy 5) to address the increased consequences of potential fires. Importantly, applying these strategies not only reduces fire probability by up to 90% but also strengthens the feedback loops and interconnections within the mine system, improving its overall resilience. Even if one subsystem fails, enhanced linkages ensure that safety can still be maintained, underscoring the importance of a systems engineering approach to fire prevention in underground mines.

4. Conclusion

This study concludes that the integration of BEVs into underground mining improves sustainability but introduces new fire safety risks driven by thermal, mechanical, electrical, and operational stress factors. Battery fault probability was found to be highly sensitive to excessive CT, extreme DoD, elevated temperatures, and battery aging, with scenario-based results showing probabilities ranging from 0.27 to 0.84 even under identical battery technology. Diesel-dominant fleets exhibited lower overall battery-related risk but higher temperature-driven hazards, while BEV-dominant fleets experienced increased electrochemical and operational stress, emphasizing the need for tailored mitigation strategies rather than uniform safety policies.

Sensitivity analysis indicated that fire risk is more sensitive to temperature increases than to traffic-related operational stresses (long CTs) or extreme DoD.

The IMF developed in this work demonstrated that multi-layered prevention strategies significantly reduce fire probability, with component-level improvements lowering risk by approximately 20%, predictive and corrective maintenance measures achieving 70–80% reduction, and the addition of emergency preparedness strategies reducing risk up to 99%. Network-based analysis showed that the mine safety system is highly sensitive to the failure of a small number of critical nodes, confirming the presence of vulnerable structural pathways that traditional static assessments tend to overlook.

While these findings are derived from the TRM case, the underlying system interactions and feedback-driven risk mechanisms are not site-specific. To ensure that the proposed framework can be applied across different underground mines, a structured adaptation approach is required.

To support transfer of the IMF beyond TRM, and to enable future development of a generalized, scientifically parameterized framework based on the stock-flow diagram, a modular and sequential adaptation protocol is proposed. Step 1 develops a qualitative understanding of site-specific feedback structures using expert input and documentation to identify key fire-risk drivers. Step 2 quantifies battery stressors through physics-based simulations or historical data, incorporating mine geometry, equipment, schedules, and environmental conditions. Step 3 converts deterministic outputs into probabilistic inputs using fitted distributions within a dynamic modeling framework. Step 4 validates model behavior against operational experience and applies sensitivity analysis to identify dominant parameters. Step 5 integrates qualitative and quantitative insights to evaluate and prioritize fire-risk mitigation strategies. This protocol enables consistent yet site-specific IMF implementation across diverse underground operations.

These findings establish that battery fire risk in electrified mines is an emergent systems-level behavior influenced by interacting operational and environmental feedbacks rather than isolated component failures. The IMF provides a decision-support basis for determining optimal prevention strategies under varying fleet compositions. Strategies 3 and 4 are the most effective in diesel-dominant fleets, and Strategy 5 is the most effective in BEV-dominant fleets for TRM.

While the estimated percentage reductions represent modeled outcomes and require real-world validation, the results highlight the need for future field-based studies and operational data integration to confirm model assumptions and support the development of robust, system-level strategies for minimizing BEV-related fire risks and strengthening mine safety resilience during the transition to electrified operations.

Funding source

This research was carried out as part of a project funded by the National Institute for Occupational Safety and Health, titled "Digital Technologies to Improve Mine Safety and Health, grant number 0000HCCR-2019–36403".

CRediT authorship contribution statement

Sultan Elcin Eroglu: Writing – original draft, Methodology. **Muhammed Kahraman:** Methodology. **H. Sebnem Duzgun:** Writing – review & editing, Supervision.

Declaration of competing interest

The authors have no competing interests to declare that are relevant to the content of this article.

Data availability

The authors do not have permission to share data.

References

[1] M. Chen, "Transitioning to battery electric vehicles in mining," 2023. Accessed: Oct. 05, 2025. [Online]. Available: https://blog.3ds.com/brands/geovia/transitioning-to-battery-electric-vehicles-mining/.
[2] Leonida C. Battery-electric vehicles: brightening the mining industry's future. Eng Min J 2020;221:32–7.
[3] Goodbody A. "Leading the electric charge,". Mining Magazine,; 2019. Accessed: Oct. 05, 2025. [Online]. Available: https://www.miningmagazine.com/technology/news/1367201/leading-electric-charge.
[4] Togun H, et al. Development and comparative analysis between battery electric vehicles (BEV) and fuel cell electric vehicles (FCEV). Appl Energy 2025;388:125726. https://doi.org/10.1016/j.apenergy.2025.125726.
[5] Alanazi F. Electric vehicles: benefits, challenges, and potential solutions for widespread adaptation. Appl Sci 2023;13(10):6016. https://doi.org/10.3390/app13106016.
[6] Halim A, Lööw J, Johansson J, Gustafsson J, van Wageningen A, Kocsis K. Improvement of working conditions and opinions of mine workers when battery electric vehicles (BEVs) are used instead of diesel machines–Results of field trial at the Kittilä mine, Finland. Min Metall Explor 2022;39(2):203–19. https://doi.org/10.1007/s42461-021-00506-8.
[7] Eroglu SE, Duzgun HS. System safety approach for the risk assessment of lithium-ion battery fires in underground mines. Fire Technol 2025. https://doi.org/10.1007/s10694-025-01745-7.
[8] Said KO, Ray A, Kumar AR. A perspective on the safety of large-format lithium-ion battery in underground mining operations: thermal runaway and its mitigation. Int J Coal Sci Technol 2025;12(1):72. https://doi.org/10.1007/s40789-025-00799-w.
[9] Eroglu SE, Duzgun HS. Investigating the Aracoma Alma Mine fire and SOMA Mine Disaster with the causal analysis based on systems theory: a comparative study. J Ind Saf 2025;2(1):7–17. https://doi.org/10.1016/j.jinse.2024.11.001.
[10] Feng X, Ouyang M, Liu X, Lu L, Xia Y, He X. Thermal runaway mechanism of lithium-ion battery for electric vehicles: a review. Energy Storage Mater 2018;10:246–67. https://doi.org/10.1016/j.ensm.2017.05.013.
[11] Bala BK, Arshad FM, Noh KM. System dynamics. Singapore: Springer Singapore; 2017. https://doi.org/10.1007/978-981-10-2045-2.
[12] Y.S. Karikari and H. Askari-Nasab, A comprehensive simulation model for mining operations: development, implementation, and validation using haulsim, n.d. Accessed: Oct. 05, 2025. [Online]. Available: https://sites.ualberta.ca/dept/civeng/mol/DataFiles/2024_Papers/403_Karikari.pdf.
[13] Howden, "Ventsim design user guide," n.d. Accessed: Oct. 05, 2025. [Online]. Available: https://ventsim.com/files/VentsimManual.pdf.
[14] He S, Shi S, Li M, Lin Z, Lu Y, Li H. Model of safety investment optimization in chemical industrial parks based on system dynamics. Reliab Eng Syst Saf 2025;256:110761. https://doi.org/10.1016/j.ress.2024.110761.
[15] Selivanova A, Krejčí I, Sedlářová-Nehézová T, Hůlka J, Češpírová I, Kuča P. Creation of a system dynamics model of recovery of affected areas after radioactive contamination. Reliab Eng Syst Saf 2025;260:111031. https://doi.org/10.1016/j.ress.2025.111031.
[16] Ma F, Zhang Y, Liu Q, Guo Y, Yang Z, Zhang J. Modeling urban transportation safety resilience under extreme rainstorms: a catastrophe theory approach. Reliab Eng Syst Saf 2025;263:111301. https://doi.org/10.1016/j.ress.2025.111301.
[17] Čepin M, Mavko B. A dynamic fault tree. Reliab Eng Syst Saf 2002;75(1):83–91. https://doi.org/10.1016/S0951-8320(01)00121-1.

[18] Nejad HS, Parhizkar T, Mosleh A. Automatic generation of event sequence diagrams for guiding simulation based dynamic probabilistic risk assessment (SIMPRA) of complex systems. Reliab Eng Syst Saf 2022;222:108416. https://doi.org/10.1016/j.ress.2022.108416.
[19] Sperstad IB, Kjølle GH, Gjerde O. A comprehensive framework for vulnerability analysis of extraordinary events in power systems. Reliab Eng Syst Saf 2020;196:106788. https://doi.org/10.1016/j.ress.2019.106788.
[20] Provan DJ, Woods DD, Dekker SWA, Rae AJ. Safety II professionals: how resilience engineering can transform safety practice. Reliab Eng Syst Saf 2020;195:106740. https://doi.org/10.1016/j.ress.2019.106740.
[21] Leveson NG. Applying systems thinking to analyze and learn from events. Saf Sci 2011;49(1):55–64. https://doi.org/10.1016/j.ssci.2009.12.021.
[22] Wen H, Khan F, AbouRizk S, Fu G. Understanding of causality and its mathematical representation in accident modeling. Reliab Eng Syst Saf 2024;250:110283. https://doi.org/10.1016/j.ress.2024.110283.
[23] Jiang H, Simonovic SP, Yu Z, Wang W. A system dynamics simulation approach for environmentally friendly operation of a reservoir system. J Hydrol 2020;587:124971. https://doi.org/10.1016/j.jhydrol.2020.124971.
[24] He S, Shi S, Li M, Lin Z, Lu Y, Li H. Model of safety investment optimization in chemical industrial parks based on system dynamics. Reliab Eng Syst Saf 2025;256:110761. https://doi.org/10.1016/j.ress.2024.110761.
[25] Amadei B. A systems approach to modeling the water-energy-land-food nexus: system dynamics modeling and dynamic scenario planning, II. New York: Momentum Press; 2019. volume II.
[26] Lu Y, Zhang SG, Hao L, Huangfu HY, Sheng H. System dynamics modeling of the safety evolution of blended-wing-body subscale demonstrator flight testing. Saf Sci 2016;89:219–30. https://doi.org/10.1016/j.ssci.2016.06.018.
[27] Cooke DL. A system dynamics analysis of the Westray mine disaster. Syst Dyn Rev 2003;19(2):139–66. https://doi.org/10.1002/sdr.268.
[28] C. Fiddes, J. Langhans, P. Schmiesing, J. Becker, T. Webber, and S. Bottoms, "NI 43-101 technical report on the Turquoise Ridge Complex Humboldt County, Nevada, USA," 2024.
[29] C.L. Bolin, S. Yopps, C. Fiddes, J. Olcott, and S.W. Yopps, "Prepared for and newmont corporation barrick gold corporation by Nevada Gold Mines LLC qualified persons: technical report on the turquoise ridge complex, State Of Nevada, USA NI 43-101 report," 2020.
[30] MSHA, "MSHA ventilation and escape map," 2022.
[31] Eds.. In: Ben-Daya M, Duffuaa SO, Raouf A, Knezevic J, Ait-Kadi D, editors. Handbook of maintenance management and engineering. London: Springer London; 2009. https://doi.org/10.1007/978-1-84882-472-0.
[32] MSHA, "Examinations of working places in metal and nonmetal mines," n.d. Accessed: Oct. 05, 2025. [Online]. Available: https://www.msha.gov/examinations-working-places-metal-and-nonmetal-mines#:~:text=A%20competent%20person%20examine%20each,a%20copy%20provided%20upon%20request.
[33] MSHA, "Mine inspections," n.d. Accessed: Oct. 05, 2025. [Online]. Available: https://www.msha.gov/compliance-and-enforcement/mine-inspections#:~:text=Citation%20&%20Order%20Writing%20Handbook,list%20of%20Frequently%20Asked%20Questions.).
[34] Node degree and strength. Fundamentals of brain network analysis. Elsevier; 2016. p. 115–36. https://doi.org/10.1016/B978-0-12-407908-3.00004-2.
[35] "Python | clustering, connectivity and other graph properties using Networkx," n.d. Accessed: Jul. 22, 2025. [Online]. Available: https://www.geeksforgeeks.org/python/python-clustering-connectivity-and-other-graph-properties-using-networkx/).
[36] "NetworkX analysis in Python," n.d. Accessed: Jul. 22, 2025. [Online]. Available: https://networkx.org/documentation/stable/reference/index.html.
[37] "Strongly connected components (SCC) in Python," n.d. Accessed: Jul. 22, 2025. [Online]. Available: https://www.geeksforgeeks.org/dsa/strongly-connected-components-scc-in-python/.
[38] Bedru HD, et al. Big networks: a survey. Comput Sci Rev 2020;37:100247. https://doi.org/10.1016/j.cosrev.2020.100247.
[39] L. Pan, "What is the optimal SOC for storing lithium-ion batteries," 2025. Accessed: Oct. 05, 2025. [Online]. Available: https://www.large-battery.com/blog/optimal-soc-for-lithium-ion-battery-storage/#:~:text=Storing%20lithium%2Dion%20batteries%20at%20a%20mid%2Dlevel%20state%20of,increases%20the%20risk%20of%20failure.
[40] Meng D, Wang X, Chen M, Wang J. Effects of environmental temperature on the thermal runaway of lithium-ion batteries during charging process. J Loss Prev Process Ind 2023;83:105084. https://doi.org/10.1016/j.jlp.2023.105084.
[41] B. Huff, "Heat generation in battery electric underground Haul trucks," 2025.
[42] L. Pan, "How heat alters lithium battery performance and lifespan," 2025. Accessed: Oct. 05, 2025. [Online]. Available: https://www.large-battery.com/blog/how-heat-alters-lithium-battery-performance-and-lifespan/#:~:text=to%20High%20Temperatures-,2.1%20Accelerated%20Aging%20and%20Shortened%20Lifespan%20of%20Battery%20Packs,and%20monitor%20battery%20storage%20conditions.).
[43] MSHA, "Heat stress," n.d. Accessed: Oct. 05, 2025. [Online]. Available: https://www.msha.gov/safety-and-health/safety-and-health-materials/heat-stress.
[44] D. Murden, "LiFePO4 battery operating temperature range: safety, precautions, and common mistakes," 2023. Accessed: Oct. 05, 2025. [Online]. Available: https://ecotreelithium.co.uk/news/lithium-iron-phosphate-battery-operating-temperature-range/.
[45] Vetter J, et al. Ageing mechanisms in lithium-ion batteries. J Power Sources 2005;147(1–2):269–81. https://doi.org/10.1016/j.jpowsour.2005.01.006.
[46] Modarres M, Kaminskiy M, Krivtsov V. Reliability engineering and risk analysis: a practical guide. CRC, CRC Press is an imprint of the Taylor and Francis Group, an information business/CRC Press, Taylor & Francis Group; 2017.
[47] Ross SM. Introduction to probability models. Academic Press; 2014.
[48] M. Hughes, "How the Weibull distribution is used in reliability engineering," 2019. Accessed: Oct. 05, 2025. [Online]. Available: https://www.allaboutcircuits.com/technical-articles/how-the-Weibull-distribution-is-used-in-reliability-engineering/.
[49] Sandvik, "Batteries for the underground load and haul," 2025.
[50] "Poisson processes," n.d. Accessed: Oct. 05, 2025. [Online]. Available: https://galton.uchicago.edu/~lalley/Courses/312/PoissonProcesses.pdf.
[51] National Fire Protection Association. NFPA 551 guide for the evaluation of fire risk assessments. National Fire Protection Association; 2022. 2022nd ed.Accessed: Mar. 12, 2025. [Online]. Available: https://link.nfpa.org/publications/551/2022.
[52] Ghiji M, et al. A review of lithium-ion battery fire suppression. Energies 2020;13(19):5117. https://doi.org/10.3390/en13195117.